

การแตกตัวของบิวเทนโดยใช้ตัวเร่งปฏิกิริยา ZSM-5 ที่ถูกปรับปรุง



นายปิยะนันท์ ผมทอง

ศูนย์วิจัยทรัพยากร

วิทยานิพนธ์นี้เป็นส่วนหนึ่งของการศึกษาตามหลักสูตรปริญญาวิศวกรรมศาสตรมหาบัณฑิต

สาขาวิชาวิศวกรรมเคมี ภาควิชาวิศวกรรมเคมี

คณะวิศวกรรมศาสตร์ จุฬาลงกรณ์มหาวิทยาลัย

ปีการศึกษา 2551

ลิขสิทธิ์ของจุฬาลงกรณ์มหาวิทยาลัย

CATALYTIC CRACKING OF BUTANE ON MODIFIED ZSM-5 CATALYST



Mr. Piyanun Phomthong

A Thesis Submitted in Partial Fulfillment of the Requirements
for the Degree of Master of Engineering Program in Chemical Engineering

Department of Chemical Engineering

Faculty of Engineering

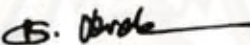
Chulalongkorn University

Academic Year 2008


Copyright of Chulalongkorn University


Thesis Title CATALYTIC CRACKING OF BUTANE ON MODIFIED
 ZSM-5 CATALYST
By Mr. Piyanun Phomthong
Field of Study Chemical Engineering
Advisor Suphot Phatanasri, D.Eng.
Co-Advisor Professor Piyasan Prasertthdam, Dr.Ing.

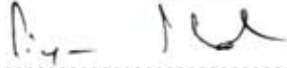
Accepted by the Faculty of Engineering, Chulalongkorn University in Partial
Fulfillment of the Requirements for the Master's Degree

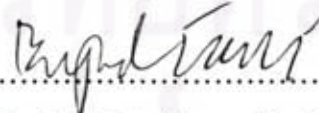

..... Dean of the Faculty of Engineering
(Associate Professor Boonsom Lerthirunwong, Dr.Ing.)

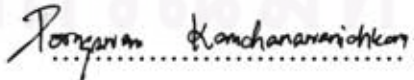
THESIS COMMITTEE


..... Chairman
(Associate Professor Paisan Kittisupakorn, Ph.D.)


..... Advisor
(Suphot Phatanasri, D.Eng.)


..... Co-Advisor
(Professor Piyasan Prasertthdam, Dr.Ing.)


..... Examiner
(Assistant Professor Bunjerd Jongsomjit, Ph.D.)


..... External Examiner
(Pornsawan Kanchanawanichkun, D.Eng.)

ปิยะนันท์ ผมทอง: การแตกตัวของบิวเทนโดยใช้ตัวเร่งปฏิกิริยา ZSM-5 ที่ถูกปรับปรุง
 CATALYTIC CRACKING OF BUTANE ON MODIFIED ZSM-5
 CATALYST อ.ที่ปรึกษาวิทยานิพนธ์หลัก: ดร.สุพจน์ พัฒนะศรี อ.ที่ปรึกษาวิทยานิพนธ์ร่วม:
 ศ.ดร. ปิยะสาร ประเสริฐธรรม, 84 หน้า

งานวิจัยนี้มีวัตถุประสงค์เพื่อทำการศึกษาผลของการปรับปรุง ZSM-5 โดยมีวิธีการเตรียมด้วยกัน 2 แบบ คือ วิธีเตรียมแบบ SOLID STATE ION EXCHANGE และ วิธีเตรียมแบบ INCIPIENT WETNESS IMPREGNATION โดยการเติมฟอสฟอรัสและแมกนีเซียมลงไปใน H/ZSM-5 ต่อประสิทธิภาพในการสังเคราะห์โอเลฟินเบาจากบิวเทน โดยการสังเคราะห์ตัวเร่งปฏิกิริยา H/ZSM-5 zeolite ที่อัตราส่วน Si/Al เป็น 40, 70 และ 100 โดยวิธีไฮโดรเทอร์มอล ตัวเร่งปฏิกิริยาที่สังเคราะห์ได้ถูกทดสอบประสิทธิภาพในช่วงอุณหภูมิ 400-700 องศาเซลเซียส เพื่อหาตัวเร่งปฏิกิริยาและอุณหภูมิในการทำปฏิกิริยาที่เหมาะสม โดยเมื่อเทียบกับปริมาณโอเลฟินเบาที่เกิดขึ้นพบว่าตัวเร่งปฏิกิริยา H/ZSM zeolite ที่อัตราส่วน Si/Al เท่ากับ 70 เป็นตัวเร่งปฏิกิริยาที่เหมาะสมและอุณหภูมิที่เหมาะสมสำหรับการเปลี่ยนบิวเทนเป็นโอเลฟินเบาคือที่ 600 องศาเซลเซียส จากนั้นนำ H/ZSM zeolite มาดัดแปลงโดยการเติมฟอสฟอรัสและแมกนีเซียมลงไปใน H/ZSM-5 ในปริมาณที่ต่างๆ กัน (0.1, 0.5 และ 3.0 เปอร์เซ็นต์โดยน้ำหนัก)โดยวิธีการ SOLID STATE ION EXCHANGE และ INCIPIENT WETNESS IMPREGNATION พบว่า วิธีการ ทั้ง 2 แบบ ที่มีการเติมสารชนิดเดียวกันนั้น ให้ผลของโอเลฟินเบาที่พอๆ กัน แต่เมื่อพิจารณาที่ตัวสารที่เติมแล้วพบว่าฟอสฟอรัสมีผลต่อการเลือกเกิดของโอเลฟินเบาที่ต่ำกว่าแมกนีเซียมเนื่องจากฟอสฟอรัสทำให้ H/ZSM zeolite มีการกระจายตัวที่ต่ำกว่าการเติมแมกนีเซียม ในขณะที่การเติมแมกนีเซียมก็ทำให้เกิดการ blocked pore ของ H/ZSM zeolite อย่างเห็นได้ชัดเจน

ภาควิชา..... วิศวกรรมเคมี..... ลายมือชื่อนิสิต..... *ปิยะนันท์ ผมทอง*
 สาขาวิชา..... วิศวกรรมเคมี..... ลายมือชื่อ อ.ที่ปรึกษาวิทยานิพนธ์หลัก..... *สุพจน์ พัฒนะศรี*
 ปีการศึกษา..... 2551..... ลายมือชื่อ อ.ที่ปรึกษาวิทยานิพนธ์ร่วม..... *ปิยะสาร ประเสริฐธรรม*

#4870383721: MAJOR CHEMICAL ENGINEERING

KEYWORDS: MODIFIED ZSM-5 / BUTANE CRACKING

PIYANUN PHOMTHONG: CATALYTIC CRACKING OF BUTANE ON MODIFIED ZSM-5 CATALYST. ADVISOR: SUPHOT PHATANASRI, D.Eng., CO-ADVISOR: PROF. PIYASAN PRASERTHDAM, Dr.Eng., 84 pp.

Light olefins synthesis from butane was investigated on H-ZSM-5 modified with phosphorus or magnesium. The effect of introduction of phosphorus or magnesium was also studied using incipient wetness impregnation and solid state ion exchange. H-ZSM-5 with Si/Al ratios of 40, 70 and 100 were hydro thermally synthesized, and the catalytic performances were examined during 400 – 700 °C. The H-ZSM-5 with Si/Al ratio of 70 exhibited the relatively high light olefins yield at 600 °C. Further modification of the catalyst was made by introduction P or Mg ranging from 0.1 – 3.0 % by weight via incipient wetness impregnation and solid state ion exchange. The introduction method gave significantly indifferent yield of light olefins for each of P and/or Mg. However, H-ZSM-5 modified with P exhibited relatively higher light olefins yield than did Mg. The better dispersion of P-modified ZSM-5 observed from SEM images should be responsible for the good catalytic performance. On the other hand, the adverse effect of Mg may be attributed to the pore blockage as clearly demonstrated by SEM and micro pore results.

Department:....Chemical Engineering . Student's Signature..... *Piyanun Phomthong*.....

Field of Study:..Chemical Engineering.. Advisor's Signature..... *Suphot Phatanasri*.....

Academic Year:.....2008..... Co-Advisor's Signature..... *Piyasan Praserttham*.....

ACKNOWLEDGEMENTS

I would like to give special recognition to Dr. Suphot Phatanasri, my advisor and Professor Piyasan Praserttham, my co-advisor for their invaluable suggestion and highly constructive comments.

I wish also to thanks to Associate Professor Paisan Kittisupakorn, chairman of the committee, Assistant Professor Bunjerd Jongsomjit and Dr. Pornsawan Kanchanawanichkun, who were members of the examining committee are acknowledged for their spending time in review my thesis and for their criticism and advice on my work.

This thesis would not be possible without the kind assistance from Assistant Professor Joongjai Panpranot, Assistant Professor Okorn Mekasuvandamrong and Dr. Aticha Chaisuwan, who always provide the encouragement and co-operate along the thesis study.

Sincere thanks are given to the graduate school and department of chemical engineering at Chulalongkorn University for the financial support of this work. Many thanks are given to Chulalongkorn University Alumni Association Under The Patronage Of His Majesty The King scholarships for supported my semester fees in 2nd, 3rd and 4th years.

Finally, I would like to manifest my greatest gratitude to my parent and many friends in Center of Excellence on Catalysis and Catalytic Reaction Engineering for their tremendous support and overwhelming encouragement, which embodied the completion of this work.

จุฬาลงกรณ์มหาวิทยาลัย

CONTENTS

	Page
ABSTRACT (THAI).....	iv
ABSTRACT (ENGLISH).....	v
ACKNOWLEDGEMENTS.....	vi
CONTENTS.....	vii
LIST OF TABLES.....	x
LIST OF FIGURES.....	xi
 CHAPTER	
I INTRODUCTION.....	1
1.1 Rationale.....	1
1.2 Research Objectives.....	2
1.3 Research Scopes.....	2
II LITERATURE REVIEWS.....	4
III THEORY.....	8
3.1 The Structure of Zeolite.....	8
3.2 Category of Zeolite.....	10
3.3 Zeolite Active Sites.....	17
3.3.1 Acid sites.....	17
3.3.2 Generation of acid centers.....	18
3.3.3 Basic sites.....	21
3.4 Shape Selective.....	22
3.5 Zeolite Synthesis.....	23
3.6 Ethylene and Propylene.....	25
3.7 Reaction Mechanism of Butane to Ethylene and Propylene...	27
IV EXPERIMENTALS.....	28
4.1 Catalyst Preparation.....	28
4.1.1 Chemicals.....	28
4.1.2 Preparation of Na/ZSM-5.....	28
4.1.2.1 Preparation of gel precipitation and decantation solution.....	31
4.1.2.2 Crystallization.....	31

CHAPTER

4.1.2.3	Calcination.....	32
4.1.2.4	Ammonium ion-exchange.....	32
4.1.3	Magnesium and phosphorus loading.....	33
4.1.3.1	Magnesium loading by incipient impregnation method.....	33
4.1.3.2	Magnesium loading by solid state ion exchange method.....	33
4.1.3.3	Phosphorus loading by incipient impregnation method.....	33
4.1.3.4	Phosphorus loading by solid state ion exchange method.....	33
4.2	Pretreatment Condition.....	34
4.3	Characterization.....	34
4.3.1	X- Ray Diffraction analysis (XRD).....	34
4.3.2	X-Ray Fluorescence analysis (XRF).....	34
4.3.3	BET surface area measurement.....	34
4.3.4	Scanning Electron Microscopy (SEM).....	35
4.3.5	Temperature Programmed Adsorptions of Ammonia (NH ₃ -TPD).....	35
4.3.6	²⁷ Al Magnetic Angle Spinning Nuclear Magnetic Resonance (²⁷ Al CP/MAS NMR).....	35
4.4	Reaction Testing.....	35
4.4.1	Chemicals and reagents.....	35
4.4.2	Instruments and apparatus.....	36
4.4.3	Reaction method.....	37
V	RESULTS AND DISCUSSIONS.....	39
5.1	The Effect of Si/Al ratio of ZSM-5 Catalyst and Reaction Temperature.....	39
5.1.1	Characterization of the catalyst.....	39
5.1.1.1	X-Ray Diffraction (XRD).....	39
5.1.1.2	Physical properties.....	40

CHAPTER	
5.1.1.3 The acidity of catalyst.....	41
5.1.2 Catalytic reaction.....	43
5.2 The Effect of Methods, Phosphorus Loading and Magnesium Loading of Si/Al Ratio of ZSM-5 Catalyst.....	46
5.2.1 Characterization of the catalysts.....	46
5.2.1.1 X-Ray Diffraction pattern.....	46
5.2.1.2 Morphology.....	46
5.2.1.3 Physical properties.....	53
5.2.1.4 Acidity.....	54
5.2.2 Catalytic reaction.....	57
VI CONCLUSIONS AND RECOMMENDATIONS.....	65
6.1 Conclusions.....	65
6.2 Recommendations.....	66
REFERENCES.....	67
APPENDICES.....	70
APPENDIX A SAMPLE OF CALCULATIONS.....	71
A-1. Calculation of Si/Al Atomic Ratio for ZSM-5.....	71
A-2. Calculation of The Amount of Magnesium Loaded to ZSM-5 Catalyst.....	72
A-3. Calculation of The Amount of Phosphorus Loaded to ZSM-5 Catalyst.....	72
APPENDIX B CALCULATIONS OF REACTION FLOW RATE.....	74
APPENDIX C DATA OF EXPERIMENT.....	75
APPENDIX D DATA AND CALCULATION OF THE ACID SITE.....	81
APPENDIX E TETRAHEDRAL ALUMINUM OF ZSM-5 CATALYST...	83
VITAE.....	84

LIST OF TABLES

	Page
TABLE	
3.1 Structural characteristics of selected zeolites.....	12
4.1 The chemicals used in the catalyst preparation.....	28
4.2 Reagents used for the preparation of Na/ZSM-5: Si/Al = 40.....	29
4.3 Operating condition for gas chromatograph.....	36
5.1 Physical properties of various Si/Al ratios of H/ZSM-5.....	41
5.2 Acidity of various Si/Al ratios of H/ZSM-5.....	41
5.3 Physical properties of various methods and species of H/ZSM-5 catalyst....	53
5.4 The peak concentration of acid site of the various methods and species of ZSM-5 catalyst.....	54
C.1 Condition uses in Shimadzu modal GC14B.....	80



 ศูนย์วิจัยทรัพยากร
 จุฬาลงกรณ์มหาวิทยาลัย

LIST OF FIGURES

	Page
FIGURE	
3.1 TO4 tetrahedra (T=Si or Al).....	9
3.2 Secondary building units (SBU's) found in zeolite structures.....	10
3.3 Structure of ZSM-23.....	13
3.4 Structure of Faujasite.....	14
3.5 Structure of beta zeolite.....	14
3.6 Structure of beta zeolite.....	15
3.7 Structure of zeolite ZSM-12.....	15
3.8 Structure of Mordenite.....	16
3.9 Framework structure of MCM-22.....	17
3.10 Diagram of the surface of a zeolite framework.....	19
3.11 Water molecules co-ordinated to polyvalent cation are dissociated by heat treatment yielding Brønsted acidity.....	20
3.12 Lewis acid site developed by dehydroxylation of Brønsted acid site.....	20
3.13 Steam dealumination process in zeolite.....	21
3.14 The enhancement of the acid strength of OH groups by their interaction with dislodged aluminum species.....	21
3.15 Diagram depicting the three type of selectivity.....	23
3.16 Ethylene.....	25
3.17 Propylene.....	26
4.1 The preparation procedure of Na/ZSM-5 by rapid crystallization method...	30
4.2 Schematic diagram of the reaction apparatus for reaction.....	38
5.1 X-Ray diffraction pattern of commercial ZSM-5 zeolite.....	40
5.2 X-Ray diffraction patterns of H/ZSM-5 with various Si/Al ratios.....	40
5.3 The NH ₃ -TPD profiles of various Si/Al ratios of H/ZSM-5 catalysts.....	42
5.4 The effect of reaction temperature and Si/Al ratios of H/ZSM-5 catalysts on the butane conversion.....	44
5.5 The effect of reaction temperature and Si/Al ratios of H/ZSM-5 catalysts on the light olefins selectivity.....	44

FIGURE

5.6 The effect of reaction temperature and Si/Al ratios of H/ZSM-5 catalysts on the light olefins yield.....	45
5.7 X-Ray diffraction patterns of P/ZSM-5 catalysts in the solid state ion exchange method.....	47
5.8 X-Ray diffraction patterns of P/ZSM-5 catalysts in the incipient impregnation method.....	47
5.9 X-Ray diffraction patterns of Mg/ZSM-5 catalysts in the solid state ion exchange method.....	48
5.10 X-Ray diffraction patterns of Mg/ZSM-5 catalysts in the incipient impregnation method.....	48
5.11 Scanning electron micrograph of P/ZSM-5 (0.1% wt PS)x 2000.....	49
5.12 Scanning electron micrograph of P/ZSM-5 (0.1% wt PS)x 1000.....	49
5.13 Scanning electron micrograph of P/ZSM-5 (0.1% wt PI)x 2000.....	50
5.14 Scanning electron micrograph of P/ZSM-5 (0.1% wt PI)x 1000.....	50
5.15 Scanning electron micrograph of Mg/ZSM-5(0.1% wt MgS)x 2000.....	51
5.16 Scanning electron micrograph of Mg/ZSM-5 (0.1% wt MgS)x 1000.....	51
5.17 Scanning electron micrograph of Mg/ZSM-5 (0.5% wt MgI)x 2000.....	52
5.18 Scanning electron micrograph of Mg/ZSM-5 (0.5% wt MgI)x 1000.....	52
5.19 The NH ₃ -TPD profiles of P/ZSM-5 catalysts on various loading in the solid state ion exchange method.....	55
5.20 The NH ₃ -TPD profiles of P/ZSM-5 catalysts on various loading in the incipient impregnation method.....	55
5.21 The NH ₃ -TPD profiles of Mg/ZSM-5 catalysts on various loading in the solid state ion exchange method.....	56
5.22 The NH ₃ -TPD profiles of Mg/ZSM-5 catalysts on various loading in the incipient impregnation method.....	56
5.23 The effect of methods of P/ZSM-5 on butane conversion and light olefins selectivity in 0.1% wt.....	57
5.24 The effect of methods of P/ZSM-5 on butane conversion and light olefins selectivity in 0.5% wt.....	58

FIGURE

5.25 The effect of methods of P/ZSM-5 on butane conversion and light olefins selectivity in 3.0% wt.....	58
5.26 The effect of methods of Mg/ZSM-5 on butane conversion and light olefins selectivity in 0.1% wt.....	59
5.27 The effect of methods of Mg/ZSM-5 on butane conversion and light olefins selectivity in 0.5% wt.....	59
5.28 The effect of methods of Mg/ZSM-5 on butane conversion and light olefins selectivity in 3.0% wt.....	60
5.29 The effect of species of P/ZSM-5 on butane conversion and light olefins selectivity in the solid state ion exchange method.....	61
5.30 The effect of species of Mg/ZSM-5 on butane conversion and light olefins selectivity in the solid state ion exchange method.....	61
5.31 The effect of species of P/ZSM-5 on butane conversion and light olefins selectivity in the incipient impregnation method.....	62
5.32 The effect of species of Mg/ZSM-5 on butane conversion and light olefins selectivity in the incipient impregnation method.....	62
5.33 The effect of species of modified ZSM-5 on butane conversion and light olefins selectivity.....	63
C.1 The calibration curve of isobutane.....	76
C.2 The calibration curve of n-butane.....	76
C.3 The calibration curve of methane.....	76
C.4 The calibration curve of ethene.....	77
C.5 The calibration curve of propane.....	77
C.6 The calibration curve of propene.....	77
C.7 The calibration curve of isobutene.....	78
C.8 The calibration curve of benzene.....	78
C.9 The calibration curve of toluene.....	78
C.10 The calibration curve of xylene.....	79
C.11 The GC14B peaks of hydrocarbons.....	80
E.1 The signal of alumina tetrahedral could be detected at around 54 ppm.....	83

CHAPTER I

INTRODUCTION

1.1 Rationale

Nowadays propylene and ethylene is used in many products but processes for propylene production cannot meet this growing demand by the high growth rate of polypropylene use[1-2] so many researchers interest in propylene and ethylene process for study about optimize condition.

ZSM-5 (MFI) is the molecular sieve catalysts which has been important from industrial and academic points of view and have been widely applied in oil refineries, the petro-chemical industry and environmental catalysis because of their unique structures, thermal stability, acidity and shape selectivity. ZSM-5 is a medium pore high silica zeolite, it has long been tested as a fluid catalytic cracking (FCC) catalyst additive to increase the octane number of gasoline. The 10-ring intersecting channels of ZSM-5 possess peculiar tear-drop-shaped pore openings of about 0.53 x 0.56 nm[3].

Propylene processes have many technologies such as propane dehydrogenation, metathesis and catalytic cracking of C4 alkanes but propane dehydrogenation and metathesis technology have seen only limited applications [1,2,4]. Propane dehydrogenation requires a high investment, and both technologies require an opportunistic feedstock economy. the catalytic cracking of C4+ alkanes to propylene and ethylene, in which the feed can be any hydrocarbons containing sufficient amounts of C4+ alkanes, such as steam cracker by-products, low-value FCC refinery streams, or catalytically cracked naphtha and light gasoline[5-9].

จุฬาลงกรณ์มหาวิทยาลัย

1.2 Research Objectives

The objectives of this research is to investigate the characteristics and performance of difference magnesium and phosphorus loading and modified method of ZSM-5 catalysts on butane cracking to ethylene and propylene.

1.3 Research Scopes

1. Study the catalytic activity and yields of ethylene and propylene of ZSM-5 zeolite catalysts having different Si/Al ratios (40, 70, 100) in butane cracking.
2. Study the characterization of the prepared catalysts by the following methods.
 - Analyzing structure and crystallinity of catalysts by X-ray diffraction (XRD).
 - Analyzing surface areas of catalysts by Brunauer-Emmett-Teller (BET) surface areas measurement.
 - Analyzing the acidity of catalysts by NH_3 -TPD.
 - Analyzing shape and size of crystallites by Scanning Electron Microscope (SEM).
3. Investigate the performance of the prepared catalysts on mixed butane cracking to ethylene and propylene under the following condition.
 - Atmospheric pressure.
 - Reaction temperature 400-700 °C.
 - Space velocity 3000 h^{-1} .
 - Reactant feed commercial butane (iso-butane 1.2%, n-butane 1.15%, nitrogen balance).
 - The reaction products were analyzed by Gas Chromatography.

ศูนย์วิจัยทรัพยากร
จุฬาลงกรณ์มหาวิทยาลัย

This thesis is arranged as follows:

Chapter II present the literature review of previous works related to this research.

Chapter III explains basic information about zeolite, reactant, main product and reaction.

Chapter IV explains the synthesis of modified ZSM-5 to convert butane into light olefin and experimental apparatus.

Chapter V presents experimental results and discussion.

Chapter VI presents overall conclusion of this thesis and recommendations for future research.



ศูนย์วิทยทรัพยากร
จุฬาลงกรณ์มหาวิทยาลัย

CHAPTER II

LITERATURE REVIEWS

In 1972, Mobil Oil Corp. published zeolite “ZSM-5” that is the catalyst which synthesized gasoline shape-selectivity from methane (The MTG process). A lot of laboratory has been developed. Some of the more prominent studied on modified catalyst and the process performance are summarized below.

Linsheng Wang et al [10] Thermally treated HZSM-5, K and Ba modified HZMS-5 exhibit a potential to be applied in producing small olefins from light paraffins. The selectivity and the yield of small olefins can be enhanced under oxidative conditions. K and Ba loaded in HZSM-5 can enhance the dehydrogenation activity and inhibit the bimolecular hydrogen transfer activity of the catalysts.

P. Cañizares et al [11] Under the conditions studied the peculiar geometry of the one-dimensional pores of mordenite suppresses the bimolecular pathway and, hence, those metal or acid centers located inside the mordenite main channels would not be active for the n-butane isomerization. However, the bimolecular pathway is not suppressed for the ZSM-5 zeolite, despite having a smaller opening of the main channel. It seems to be clear that, due to its three-dimensional pore system, the octylcarbenium ions could be formed inside the channel intersections.

K. Wakui et al [12] In the Cracking of n-butane using alkaline earth modified HZSM-5 catalysts, the ethene and propene selectivities were improved compare with the non-modified HZSM-5, although the catalyst activities were lowered. The NH₃-TPD spectra of these catalysts showed that the strong acid sites were transformed to weak acid sites. When using the alkaline earth-modified HZSM-5, the ethane/ethane and the C₂/other product ratios were higher than those obtained using the non-modified one. It was found that the control of the acid character and the dehydrogenization activity of the HZSM-5 catalyst is important for an improvement of the olefin yield.

Guiyuan Jiang et al [13] A series of HZSM-5 zeolites modified by different amounts of phosphorus were prepared, and their performances for the catalytic cracking of the mixed C4 alkanes to produce light olefins were investigated. The results showed that the introduction of phosphorus into HZSM-5 zeolite greatly enhanced the selectivity to light olefins, especially to propylene, thus increased the total yield of olefins in the catalytic cracking of mixed C4 alkanes. At the temperature of 650 °C, the maximum yields of propene and ethene were achieved 25.6 and 33.9%, which were higher than those over parent HZSM-5 by 7 and 4.5%, respectively.

K. Wakui et al [14] During the cracking of n-butane using modified HZSM-5, it was observed that the initial selectivity of products was different from those obtained by HZSM-5. Dehydrogenation of butane was enhanced on cobalt-containing HZSM-5 catalyst and the product butane further cracked to ethylene as the reaction proceeded. With the magnesium-containing HZSM-5, the selectivity of ethylene was high although at low conversion. A different mechanism of cracking from those with Mg-ZSM-5. On the other hand, the initial cracking selectivity obtained using the lanthanum-containing HZSM-5 was almost equal to the non-modified HZSM-5. The improved olefin yield obtained using the lanthanum loaded HZSM-5 previously reported in the literature was improved not to be contributed from the initial cracking selectivity over the catalyst. It is considered that dehydrogenative-cracking is a possible alternative process for olefin production from alkanes using an appropriately designed catalyst.

Dong Ji et al [15] Therefore, owing to the increasing need for olefins (ethylene and propylene), it was reported that MFI type zeolites could be used for cracking of lighter distillate fractions from a steam cracker to increase the total yield of olefin in the process. Wakui et al. investigated cracking of n-butane with rare earth-loaded HZSM-5 and they found that the formation of aromatic and heavier products is remarkably suppressed by the loading of rare earths. In order to search for the possibilities of obtaining more ethylene and propylene by cracking using rare earth-loaded HZSM-5, they reported a dehydrogenation cracking double-stage reaction of n-butane.

Y. Guang Li et al [16] Magnesium-containing ZSM-5 catalysts were prepared via a solid state reaction of HZSM-5 zeolite with magnesium chloride at 327°C. X-ray determinations showed that structure and crystallinity of the catalysts were not changed after the solid-state reaction.

H. Krannila et al [17] The cracking of n-butane catalyzed by the zeolite HZSM-5 has been characterized by measurements of the conversion determined with a flow reactor at temperatures of 426-523°C and n-butane partial pressures of 0.01-1.00 atm. The primary products, each formed in a first-order reaction, are H₂ + butenes; methane + propylene; and ethane + ethylene. In the limit approaching zero conversion, each compound in each stated pair was formed at approximately the same rate as the other. Propane and a small amount of isobutane were formed as secondary products in secondorder reactions. The results are consistent with the occurrence of two simultaneous mechanisms: (1) a monomolecular mechanism proceeding through the pentacoordinated carbonium ion formed by protonation of the n-butane at the two position and (2) a bimolecular hydride transfer proceeding through carbenium ion intermediates. The former proceeds almost to the exclusion of the latter in the limit approaching zero n-butane conversion. The limiting product distribution characterizes the intrinsic selectivity of the collapse of the carbonium ion; at 496°C, the relative rates of decomposition of the carbonium ion to give H₂ + butenes, methane + propylene, and ethane + ethylene are 30 ± 6, 36 ± 4, and 34 ± 5, respectively, with the corresponding activation energies all being approximately 140 kJ/mol. These results provide the first demonstration of stoichiometric dehydrogenation accompanying paraffin cracking.

Costas S. Triantafillidis et al [18] The sizes of the ZSM-5 particles have a strong effect on the changes in product yields and gas and gasoline compositions. Smaller particles favor a decrease in gasoline and an increase in LPG yield more than larger particles. The effect is more pronounced in the high acidity region where the decrease in the yields of C₇+ isoalkanes, naphthenes, and aromatics is favored by small particle additives, while the effect of particle size on gasoline range hydrocarbons is clearly evident on the yields of gaseous products.

Tao Long-Xiang et al [19] A new method is presented for olefin production by oxidative dehydrogenation-cracking of light alkanes. ZSM-5 zeolites modified by Co, Mo, K, Ca, Mg, etc., were used as catalysts. The selectivity of olefins in the oxidative dehydrogenation-cracking of n-pentane and n-hexane greatly increased in comparison with that in catalytic cracking on USY-zeolites.



ศูนย์วิทยทรัพยากร
จุฬาลงกรณ์มหาวิทยาลัย

CHAPTER III

THEORY

3.1 The Structure of Zeolite

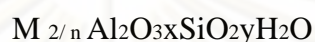
Zeolites are highly crystalline, hydrated aluminosilicates that upon dehydration develop in the ideal crystal a uniform pore structure having minimum channel diameters (aperture) of from about 0.3 to 1.0 nm. The size depends primarily on the type of zeolites and secondarily on the cations present and the nature of treatments such as calcination, leaching, and various chemical treatments. Zeolites have been of intense interest as catalysts for some three decades because of the high activity and unusual selectivity they provide, mostly in a variety of acid-catalyzed reactions. In many cases, but not all, the unusual selectivity is associated with the extremely fine pore structure, which permits only certain molecules to penetrate into the interior of the catalyst particles, or only certain products to escape from the interior. In some cases unusual selectivity seems to stem instead from constraints that the pore structure sets on allowable transition states, sometimes termed spacio-selectivity.

The structure of the zeolite consists of a three-dimensional framework of the SiO_4 and AlO_4 tetrahedra as presented in Figure 3.1 [20], each of which contains a silicon or aluminum atom in the center. In 1982, Barrer defined zeolites as the porous tectosilicates [21], that is, three-dimensional networks built up of TO_4 tetrahedra where T is silicon or aluminum. The oxygen atoms are shared between adjoining tetrahedra, which can be present in various ratios and arranged in a variety of ways. The framework thus obtained has pores, channels, and cages, or interconnected voids.

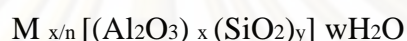
A secondary building unit (SBU) consists of selected geometric groupings of those tetrahedra. There are sixteen such building units, which can be used to describe all of the known zeolite structures; for example, 4 (S4R), 6 (S6R), and 8 (S8R) – member single rings, 4-4 (D6R), 8-8 (D8R) – member double rings. The topologies of these units are shown in Figure 3.2 [22]. Also listed are the symbols used to describe them. Most zeolite frameworks can be generated from several different SBU's. Descriptions of

known zeolite structures based on their SBU's[23]. Both ZSM-5 zeolite and Ferrierite are described by their 5-1 building units. Offertile, Zeolite L, Cancrinite, and Erionite are generated using only single 6- member rings. Some zeolite structures can be described by several buildings. The sodalite framework can be built from either the single 6-member ring or the single 4- member ring. Faujasite (type X or type Y) and zeolite be constructed using 4 ring or 6 ring building units. Zeolite a can also be formed using double 4 ring building units, whereas Faujasite cannot.

Zeolites may be represented by the empirical formula:



or by a structural formula:



Where the bracketed term is the crystallographic unit cell. The metal cation (of valence n) is present it produces electrical neutrality since for each aluminum tetrahedron in the lattice there is an overall charge of -1 . Access to the channels is limited by aperture consisting of a ring of oxygen atoms of connected tetrahedra. There may be 4, 5, 6, 8, 10, or 12 oxygen atoms in the ring. In some cases an interior cavity exists of larger diameter in the aperture; in others, the channel is of uniform diameter like a tube [24].

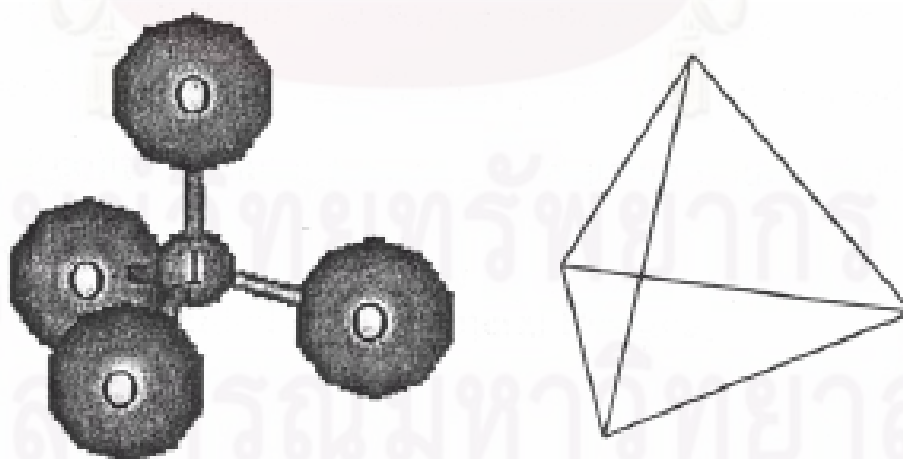


Figure 3.1 TO₄ tetrahedra (T=Si or Al) [20]

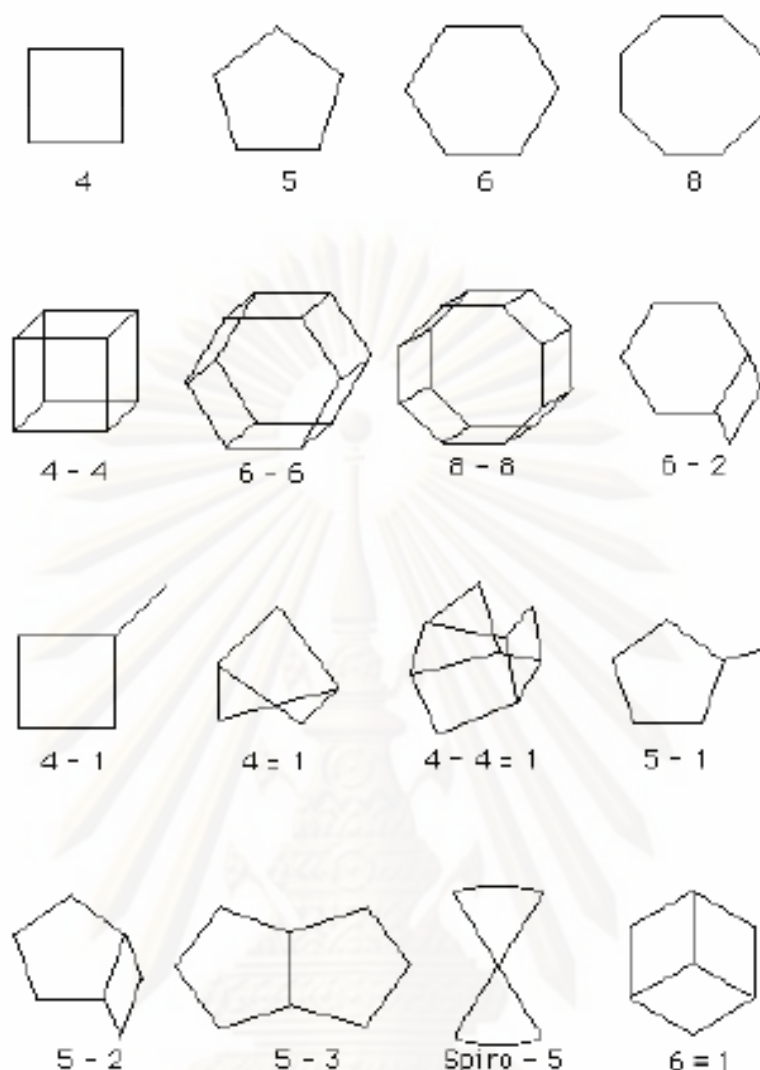


Figure 3.2 Secondary building units (SBU's) found in zeolite structures[22]

3.2 Category of Zeolite

There are over 40 known natural zeolites and more than 150 synthetic zeolites have been reported [3]. The number of synthetic zeolites with new structure morphologies grows rapidly with time. Based on size of their pore opening, zeolites can be roughly divided into five major categories, namely 8-, 10-, and 12-member oxygen ring systems, dual pore systems and mesoporous systems. Their pore structures can be characterized by crystallography, adsorption, measurements and/or through diagnostic reactions. One such diagnostic characterization test is the “constraint index” test. The concept of constraint index was defined as the ratio of the

cracking rate constant of n-hexane to 3-methylpentane. The constraint index of a typical medium-pore zeolite usually ranges from 3 to 12 and those of the large-pore zeolites are the range 1-3. For materials with an open porous structure, such as amorphous silica alumina, their constraint indices are normally less than 1. On the index for erionite is 38.

A comprehensive bibliography of zeolite structures has been published by the International Zeolite Association [3]. The structural characteristics of assorted zeolites are summarized in Table 3.2

Zeolite with 10-membered oxygen rings normally possesses a high siliceous framework structure. They are of special interest in industrial applications. In fact, they were the first family of zeolite that was synthesized with organic ammonium salts. With pore openings close to the dimensions of many organic molecules, they are particularly useful in shape selective catalysis. The 10-membered oxygen ring zeolites also possess other important characteristic properties including high activity, high tolerance to coking and high hydrothermal stability. Among the family of 10-membered oxygen ring zeolites, the MTT – type(ZSM-23) zeolite is high-silica zeolite as presented in Figure 3.3 containing 5-, 6-, and 10-ring subunits that generate undimensional 10-member-ring channels which are parallel to the short 5 Å axis. The pore opening is teardrop-shaped 10-member ring. This structure is thought to be similar that of ZSM-22 zeolite [25]

ZSM-23 zeolite was claimed to crystallize from a reactive aluminosilicate gel with a $\text{SiO}_2/\text{Al}_2\text{O}_3$ ratio between 55 and 70 with pyrrolidine as the organic additive and an OH/SiO_2 between 0.01 and 0.049. In the presence of DiQuat-7 the range of $\text{SiO}_2/\text{Al}_2\text{O}_3$ was extended to 5000. The ratio of the organic to the total cation content in the gel ranges between 0.85 and 0.95. Crystallization takes place after 5 days at 433 K, producing pure ZSM-23 zeolite. Common impurity phases, which are dependent on the amount of hydroxide or the $\text{SiO}_2/\text{Al}_2\text{O}_3$ ratio, include cristobalite and ZSM-5 zeolite(ACS Sym. Ser. 398:560(1989))

Crystallization of this structure also occurs under more acidic conditions in the presence of fluoride ion, with an F/SiO_2 ratio between 0.1 and 6 (EP 347,273(1989))

The iron-containing analog of this material also has been prepared (J.Catal. 121:89(1980))

Table 3.1 Structural characteristics of selected zeolites [3]

Zeolite	Number of rings	Pore opening Å	Pore/Channel structure	Void volume (ml/g)	D_{Frame}^a (g/ml)	CI^b
<i>8-membered oxygen ring</i>						
Erionite	8	3.6x5.1	Intersecting	0.35	1.51	38
<i>10-membered oxygen ring</i>						
ZSM-5	10	5.3x5.6 5.1x5.5	Intersecting	0.29	1.79	8.3
ZSM-11	10	5.3x5.4	Intersecting	0.29	1.79	8.7
ZSM-23	10	4.5x5.2	One-dimensional	-	-	9.1
<i>Dual pore system</i>						
Ferrierite (ZSM-35, FU-9)	10,8	4.2x5.4 3.5x4.8	One-dimensional 10:8 intersecting	0.28	1.76	4.5
MCM-22	12	7.1	Capped by 6 rings	-	-	1-3
Mordenite	10	Elliptical				
	12	6.5x7.0	One-dimensional	0.28	1.70	0.5
	8	2.6x5.7	12:8 intersecting			
Omega (ZSM-4)	12	7.4	One-dimensional	-	-	2.3
	8	3.4x5.6	One-dimensional	-	-	0.6
<i>12membered oxygen ring</i>						
ZSM-12	12	5.5x5.9	One-dimensional	-	-	2.3
Beta	12	7.6x6.4 5.5x5.5	Intersecting	-	-	0.6
Faujasite (X,Y)	12	7.4	Intersecting	0.48	1.27	0.4
	12	7.4x6.5	12:12 intersecting			
<i>Mesoporous system</i>						
VPI-5	18	12.1	One-dimensional	-	-	-
MCM41-S	-	16-100	One-dimensional	-	-	-

^aFramework density

^bConstraint index

จุฬาลงกรณ์มหาวิทยาลัย

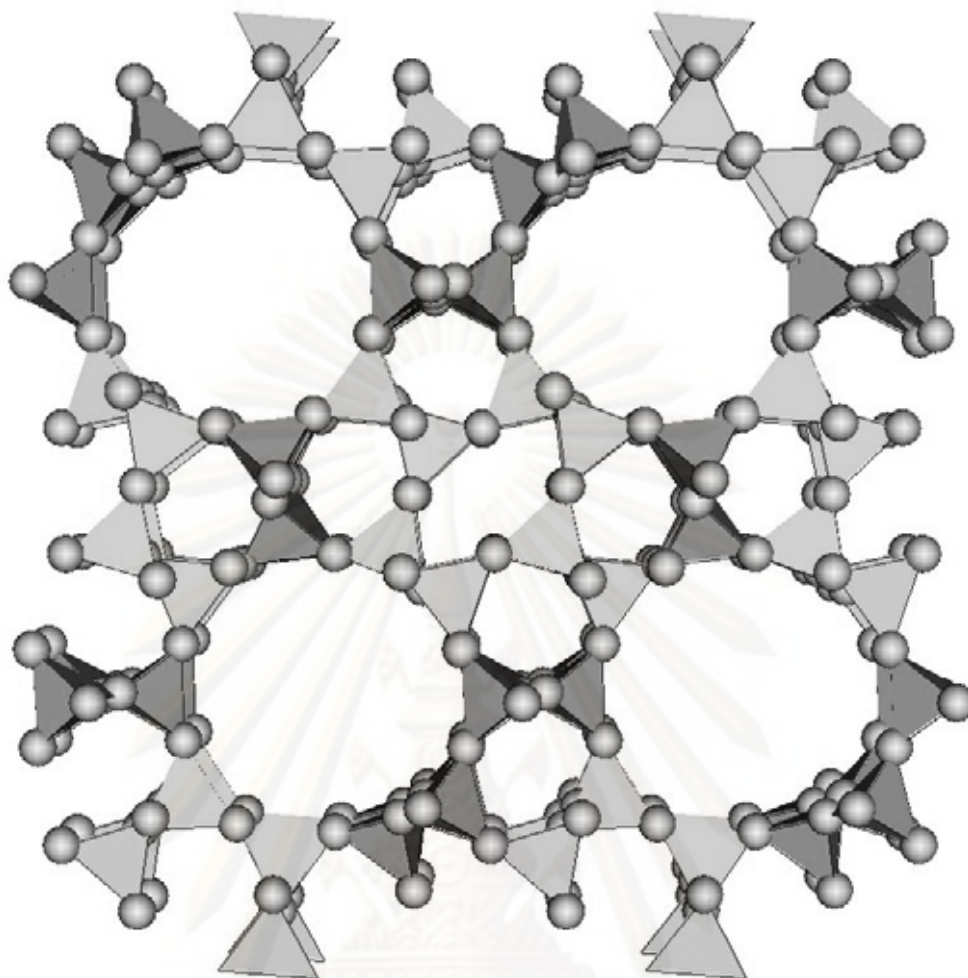


Figure 3.3 Structure of ZSM-23 (<http://www.personal.utulsa.edu/~geoffrey-price/zeolite/mtt.jpg>).

Although the 10-membered oxygen ring zeolite was found to possess remarkable shape selectivity, catalysis of large molecules may require a zeolite catalyst with a large-pored opening. Typical 12-membered oxygen ring zeolites, such as faujasite-type zeolites, normally have pore opening greater than 5.5 \AA and hence are more useful in catalytic applications with large molecules, for example in trimethylbenzene (TMB) conversions. Faujasite (X or Y; Figure 3.4 [3]) zeolites can be synthesized using inorganic salts and have been widely used in catalytic cracking since 1960s. The framework structures of beta zeolite and ZSM-12 are shown in Figure 3.5 and 3.6, respectively.

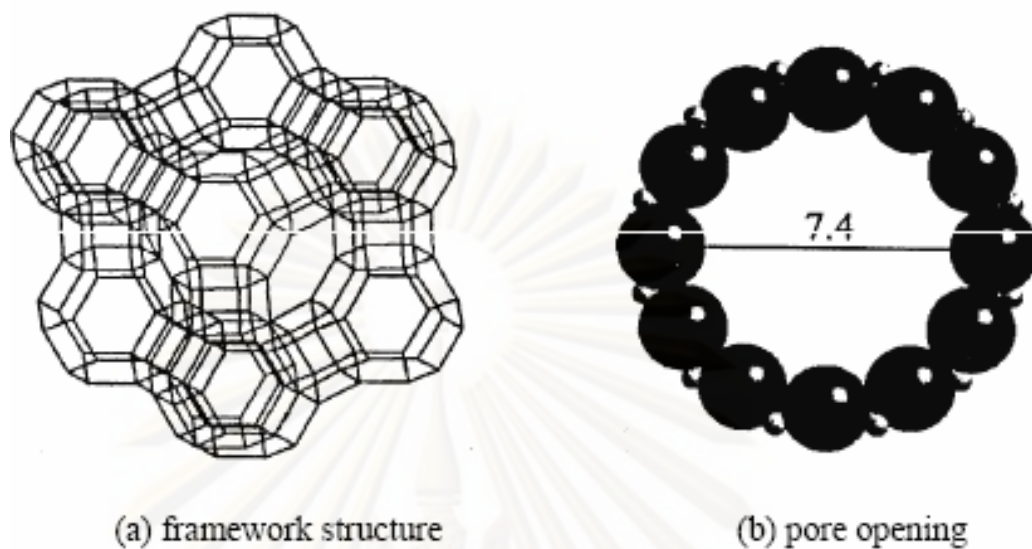


Figure 3.4 Structure of Faujasite [3].

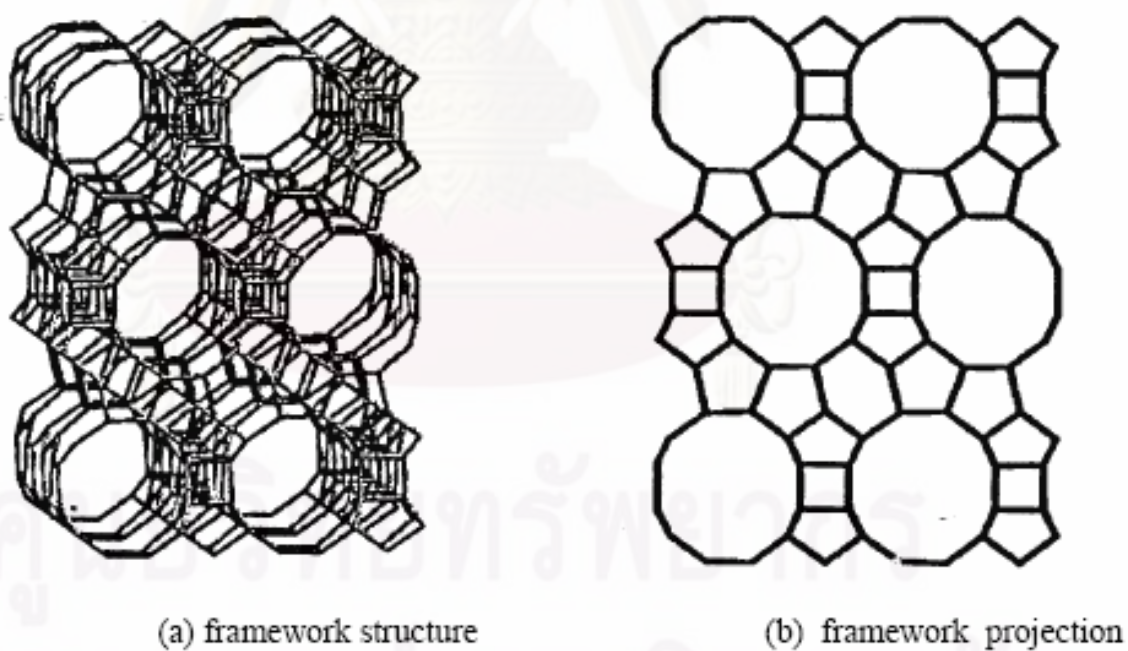


Figure 3.5 Structure of beta zeolite [3].

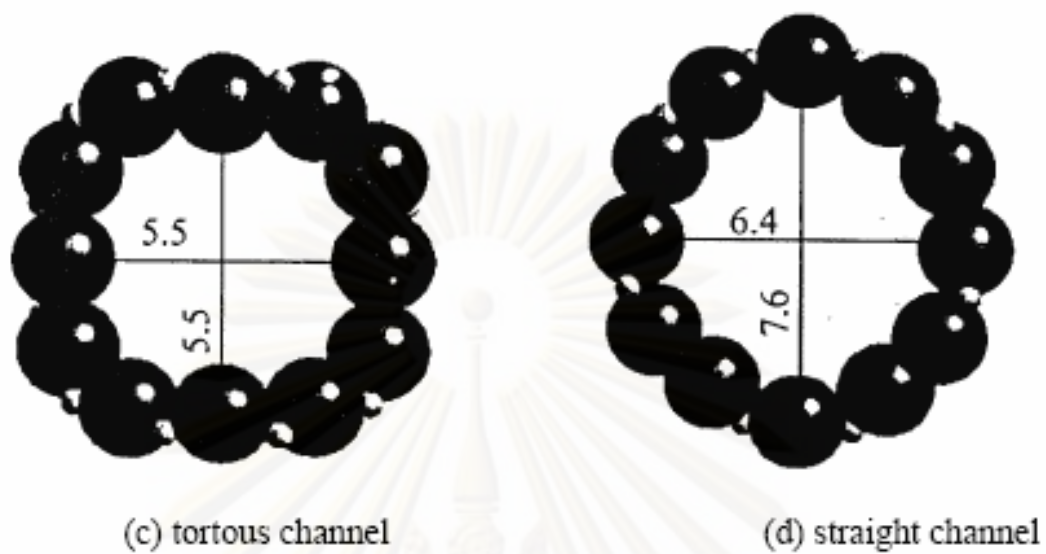


Figure 3.6 Structure of beta zeolite [3].

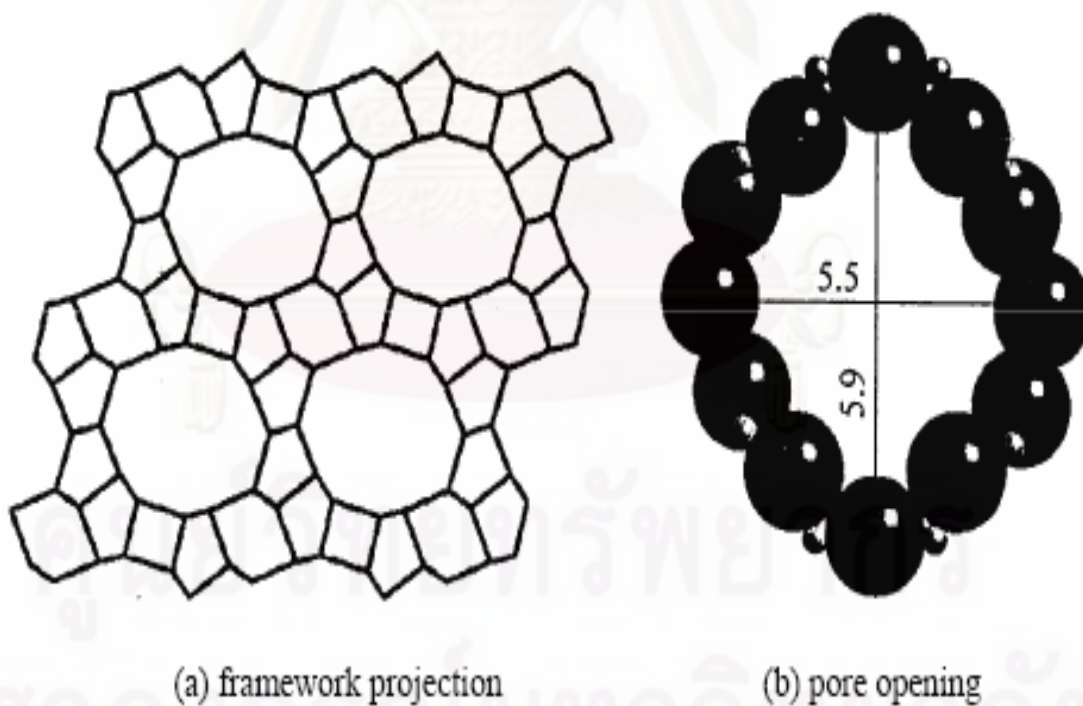


Figure 3.7 Structure of zeolite ZSM-12 [3].

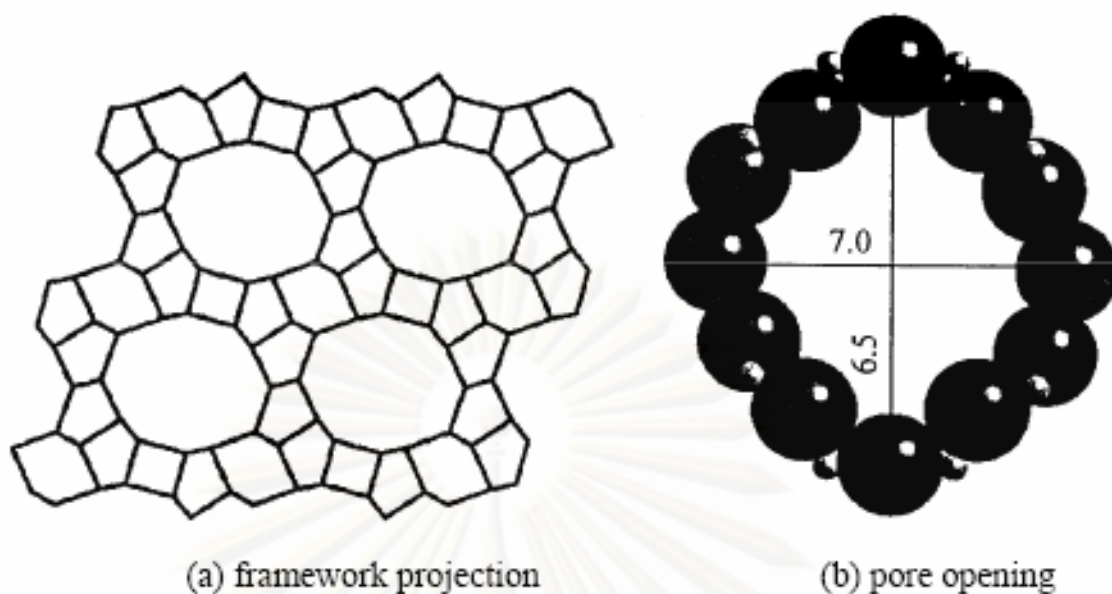


Figure 3.8 Structure of Mordenite [3].

Zeolites with a dual pore system normally possess interconnecting porechannels with two different pore opening sizes. Mordenite is a well-known dual pore zeolite having a 12-membered oxygen ring channel with pore opening $6.5 \times 6.7 \text{ \AA}$ which is interconnected to 8-membered oxygen ring channel with opening $2.6 \times 5.7 \text{ \AA}$ (Figure 3.7 [26]). MCM-22, which was found more than 10 years ago, also possesses a dual pore system. Unlike Mordenite, MCM-22 consists of 10- and 12-membered oxygen rings (Figure 3.8 [3]) and thus shows prominent potential in future applications.

In the past decade, many research efforts in synthetic chemistry have been invested in the discovery of large-pored zeolite with pore diameter greater than 12-membered oxygen rings. The recent discovery of mesoporous materials with controllable pore opening (from 12 to more than 100 \AA) such as VPI-5, MCM-41S undoubtedly will shed new light on future catalyst applications.

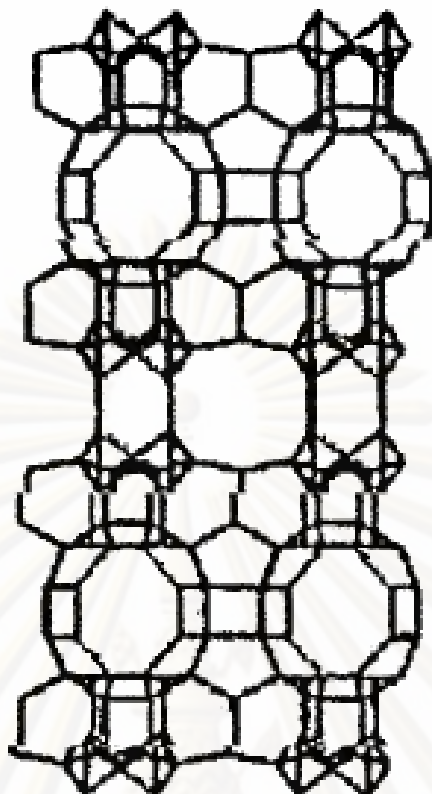


Figure 3.9 Framework structure of MCM-22 [3].

3.3 Zeolite Active Sites

3.3.1 Acid sites

Classical Brønsted and Lewis acid models of acidity have been used to classify the active sites on zeolites. Brønsted acidity is proton donor acidity; a tridiagonally coordinated aluminum atom is an electron deficient and can accept an electron pair, therefore behaves as a Lewis acid [27].

In general, the increase in Si/Al ratio will increase acidic strength and thermal stability of zeolite [28]. Since the numbers of acidic OH groups depend on the number of aluminum in zeolites framework, decrease in Al content is expected to reduce catalytic activity of zeolite. If the effect of increase in the acidic centers, increase in Al content, shall result in enhancement of catalytic activity

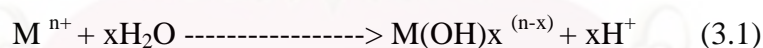
Based on electrostatic consideration, the charge density at a cation site increase with increase Si/Al ratio. It was conceived that these phenomena are related to reduction of electrostatic interaction between framework sites, and possibly to difference in the order of aluminum in zeolite crystal-the location of Al in crystal structure [29].

An improvement in thermal or hydrothermal stability has been ascribed to the lower density of hydroxyl groups, which is parallel to that of Al content [27]. A longer distance between hydroxyl groups decrease the probability of dehydroxylation that generates defects on structure of zeolites.

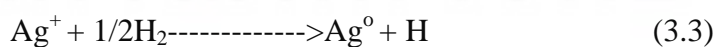
3.3.2 Generation of acid centers

Protonic acid centers of zeolite are generated in various ways. Figure 3.9 depicts the thermal decomposition of ammonium-exchanged zeolite yielding the hydrogen form [15].

The Brønsted acidity due to water ionization on polyvalent cations, described below, is depicted in Figure 3.10 (Tanaka et al., 1989).



The exchange of monovalent ions by polyvalent cations could improve the catalytic property. Those highly charged cations create very centers by hydrolysis phenomena. Brønsted acid sites are also generated by the reduction of transition metal cations. The concentration of OH groups of zeolite containing transition metals was noted to increase by hydrogen at 275.5 – 723 K to increase with the rise of the reduction temperature [20].



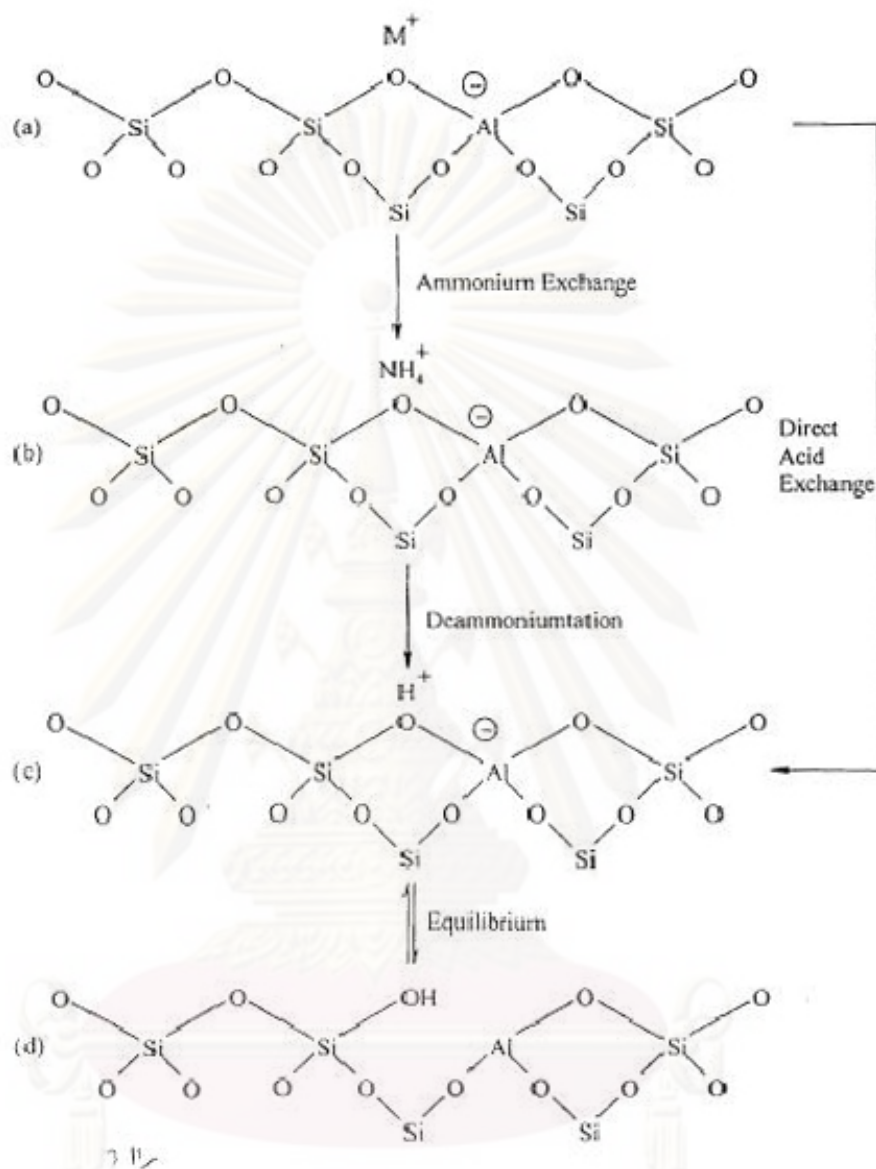


Figure 3.10 Diagram of the surface of a zeolite framework [23].

a) In the as-synthesis form M^+ either an organic cation or an alkali metal cation.

b) Ammonium in exchange produces the NH_4^+ exchanged form.

c) Thermal treatment is used to remove ammonia, producing the H^+ , acid form.

d) The acid form in (c) is in equilibrium with the shown in (d), where is a silanol group adjacent to tricoordinate aluminium.

The formation of Lewis acidity from Brønsted acid sites is depicted in Figure 3.11. The dehydration reaction decrease the number of protons and increases that of Lewis sites. Brønsted (OH) and Lewis (-Al-) sites can be present simultaneously in the structure of zeolite at high temperature. Dehydroxylation is thought to occur in ZSM-5 zeolite above at 773 K and calcination at 1073 to 1173 K produces irreversible dehydroxylation, which causes defection in crystal structure of zeolite.

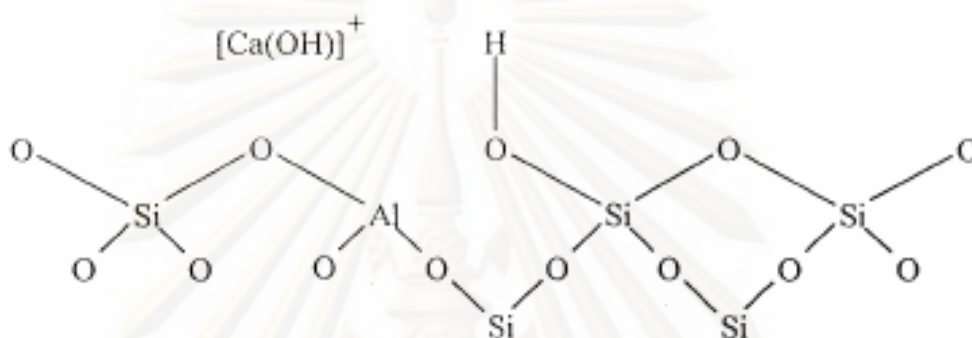


Figure 3.11 Water molecules co-ordinated to polyvalent cation are dissociated by heat treatment yielding Brønsted acidity.

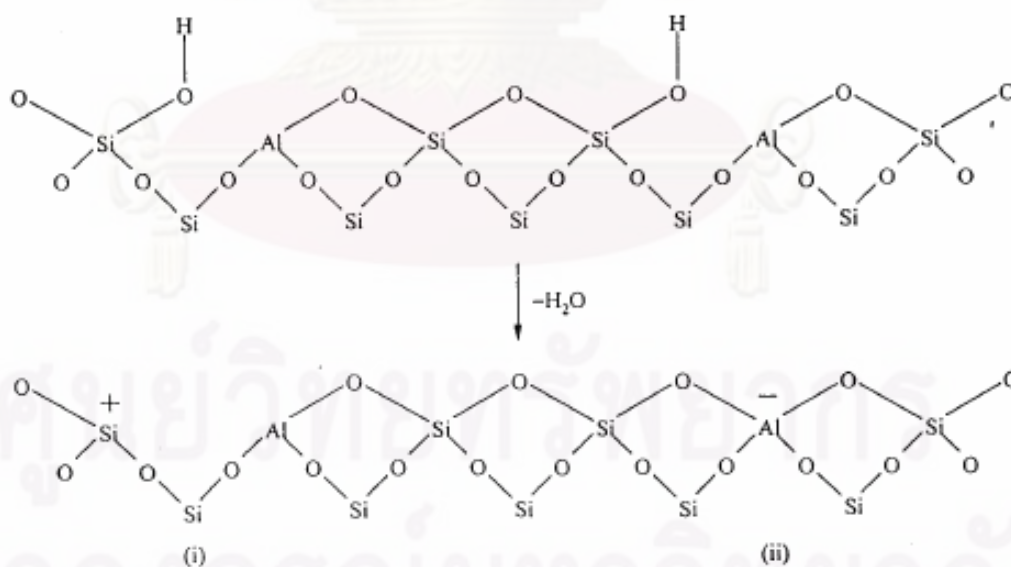


Figure 3.12 Lewis acid site developed by dehydroxylation of Brønsted acid site.

Dealumination is believed to occur during dehydroxylation, which may result from the steam generation within the sample. The dealumination is indicated by an increase in the surface concentration of aluminum on the crystal. The dealumination process is expressed in Figure 3.12 [30]. The extent of dealumination monotonously increases with the partial pressure of steam.

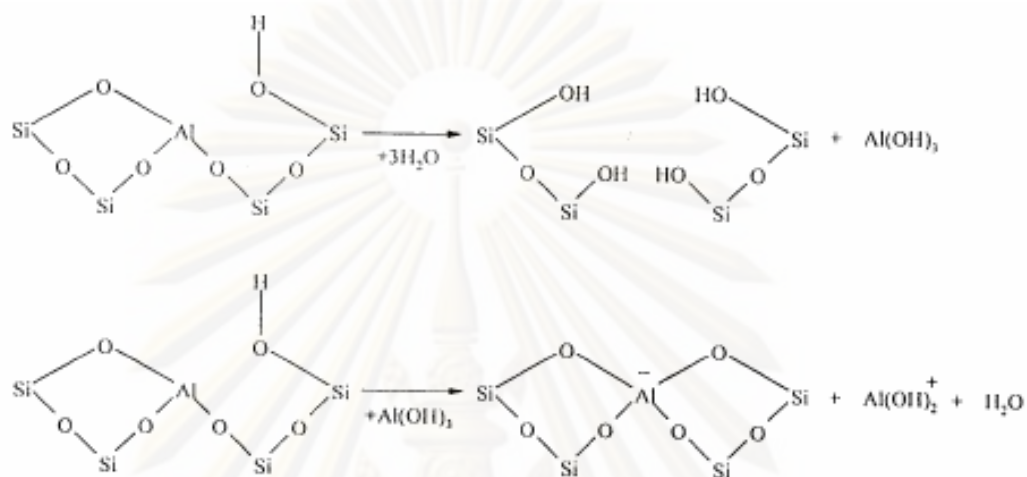


Figure 3.13 Steam dealumination process in zeolite [30]

The enhancement of the acid strength of OH groups is recently proposed to be pertinent to their interaction with those aluminum species sites tentatively expressed in Figure 3.13 [30]. Partial dealumination might therefore yield a catalyst of higher activity while severe steaming reduces the catalytic activity.

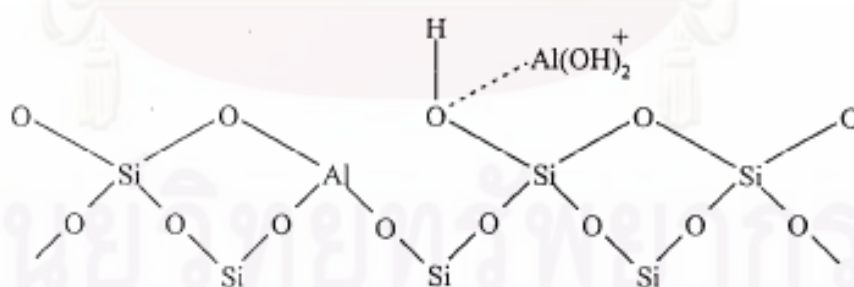


Figure 3.14 The enhancement of the acid strength of OH groups by their interaction with dislodged aluminum species [30].

3.3.3 Basic sites

In certain instances reactions have been shown to be catalyzed at basic (cation) site in zeolite without any influences from acid sites. The best-characterized example

of this is that K –Y which splits n-hexane isomers at 773 K. The potassium cation has been shown to control the unimolecular cracking (β -scission). Free radical mechanisms also contribute to surface catalytic reactions in these studies.

3.4 Shape Selective

Many reactions involving carbonium intermediates are catalyzed by acidic zeolite. With respects to a chemical standpoint the reaction mechanisms are not fundamentally different with zeolites or with any the acidic oxides. What zeolite add is shape selectivity effect. The shape selective characteristics of zeolites influence their catalytic phenomena by three modes: shape selectivity, reactants shape selectivity, products shape selectivity and transition states shape selectivity. These types of selectivity are illustrated in Figure 3.14.

Reactants of charge selectivity results from the limited diffusibility of some of the reactants, which cannot effectively enter and diffuse inside crystal pore structures of the zeolites. Product shape selectivity occurs as slowly diffusing product molecules cannot escape from the crystal and undergo secondary reaction. This reaction path is established by monitoring changes in product distribution as a function of varying contact time.

Restricted transition state shape selectivity is a kinetic effect from local environment around the active site, the rate constant for a certain reaction mechanism is reduced of the space required for formation of necessary transition state is restricted.

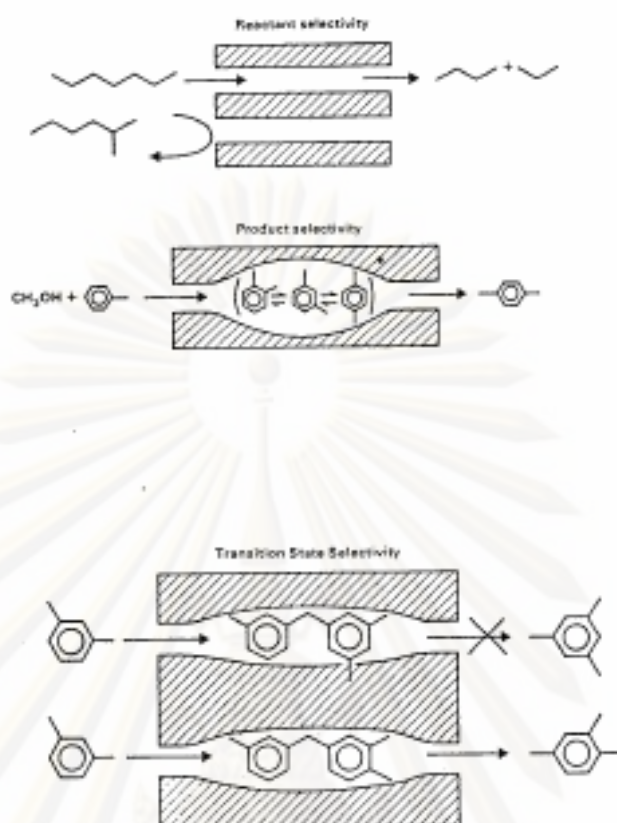


Figure 3.15 Diagram depicting the three type of selectivity [23].

The critical diameter (as opposed to the length) of the molecules and the pore channel diameter of zeolites are important in predicting shape selective effects. However, molecules are deformable and can pass through opening, which are smaller than their critical diameters. Hence, not only size but also the dynamics and structure of the molecules must be taken into account.

3.5 Zeolite Synthesis

Zeolites are generally synthesized by a hydrothermal process from a source of alumina (e.g., sodium aluminate or aluminium sulfate) and of silica (e.g., a silica sol, fumed silica, or sodium water glass) and an alkali such as NaOH, and/or a quaternary ammonium compound. An inhomogeneous gel is produced which gradually crystallizes, in some cases forming more than one type of zeolite in succession. Nucleation effects can be important, and an initial induction period at near ambient

temperature may be followed by crystallization temperature that may range up to 473 K or higher. The pressure is equal to the saturated vapor pressure of the water present.

The final product depends on a complex interplay between many variables including $\text{SiO}_2/\text{Al}_2\text{O}_3$ ratio in the starting medium, nucleating agents, temperature, pH, water content, aging, stirring, and the presence of various inorganic and organic cations. Much remains to be learned about how the initial reaction mixture forms the precursor species and how these arrange into the final crystalline products. A key concept is that the cations present give rise to a templating action, but clearly the process is more complex.

Bauer and coworkers in the early 1960s developed the use of reaction mixtures containing quaternary ammonium ions or other or other cations to direct the crystallization process. In their work and succeeding studies, a primary motivation was to attempt to synthesize zeolites with large apertures than X and Y. This did not occur, but instead organic species were found to modify the synthesis process in a variety of ways that led to the discovery of many new zeolites, and new methods of synthesizing zeolite with structures similar to previously know zeolite.

The mechanism of action of the organic species is still controversial. It was originally thought to be primarily a templating effect, but later it was found that at least some of zeolites could be synthesized without an organic template. Further, organic species other than quaternary ammonium compounds had directing effects not readily ascribed to their size or shape. However, an important result was the zeolites of higher $\text{SiO}_2/\text{Al}_2\text{O}_3$ ratio than before could be synthesized. Previously, only structures with $\text{SiO}_2/\text{Al}_2\text{O}_3$ ratios of about 10 or less could be directly forms, but with organic additives, zeolites with ratio of 20 to 100 or more can be directly prepared.

After synthesis the zeolite are washed, dried, heated to remove water of crystallization, and calcined in air, e.g., at about 813 K. Organic species are also thus removed. For most catalytic purpose, the zeolite is converted into acidic form. For some zeolites this can be achieved by treatment with aqueous HCl without significantly altering the framework structure. For other zeolites Na^+ is replaced with NH_4^+ via an ammonium compound such as NH_4OH , NH_4Cl or NH_4NO_3 . Upon heating NH_3 is driven off, leaving the zeolite in the acid form. For some reaction a

hydrogenation component such as platinum or nickel is introduced by impregnation or ion exchange [15].

3.6 Ethylene and Propylene

Ethylene is used primarily as an intermediate in the manufacture of other chemicals, especially plastics. Ethylene may be polymerized directly to produce polyethylene (also called polyethylen or polythene), the world's most widely-used plastic. Ethylene can be chlorinated to produce ethylene dichloride (1,2-Dichloroethane), a precursor to the plastic polyvinyl chloride, or combined with benzene to produce ethylbenzene, which is used in the manufacture of polystyrene, another important plastic.

Smaller amounts of ethylene are oxidized to produce chemicals including ethylene oxide, ethanol, and polyvinyl acetate. Global demand for ethylene exceeded 100 million tonnes per year in 2005. Ethylene was once used as an inhaled anesthetic, but it has long since been replaced in this role by nonflammable gases. It has also been hypothesized that ethylene was the catalyst for utterances of the oracle at Delphi in ancient Greece. Ethylene is used in greenhouses and is sprayed on crops to speed ripening. It is also found in many lip gloss products. [<http://en.wikipedia.org/wiki/Ethylene>]

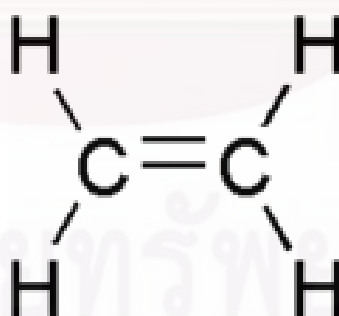


Figure 3.16 Ethylene [<http://en.wikipedia.org/wiki/Ethylene>]

Propylene, also known by its IUPAC name propylene, is an organic compound having the chemical formula C₃H₆. It is the second simplest member of the alkene class of hydrocarbons, ethylene (ethylene) being the simplest. At room temperature and pressure, propylene is a gas. It is colorless, highly flammable, and has an odor similar to garlic.(this smell is added to make it easily detectable, pure propylene, like

most simple hydrocarbons, has no natural scent.) It is found in coal gas and can be synthesized by cracking petroleum. Propylene is a major commodity in the petrochemicals industry. The main use of propylene is as a monomer, mostly for the production of polypropylene. Propylene is also used as a fuel gas for various industrial processes. It has a similar calorific value to propane but a lower mass of combustion products so a higher flame temperature. Propylene also has approximately twice the vapor pressure of propane at room temperature and pressure. [<http://en.wikipedia.org/wiki/Propylene>]

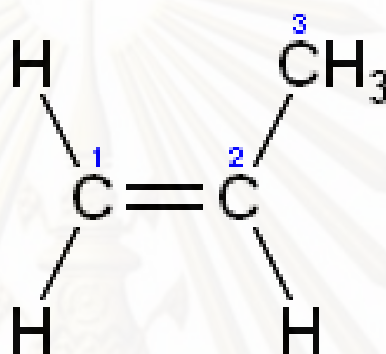
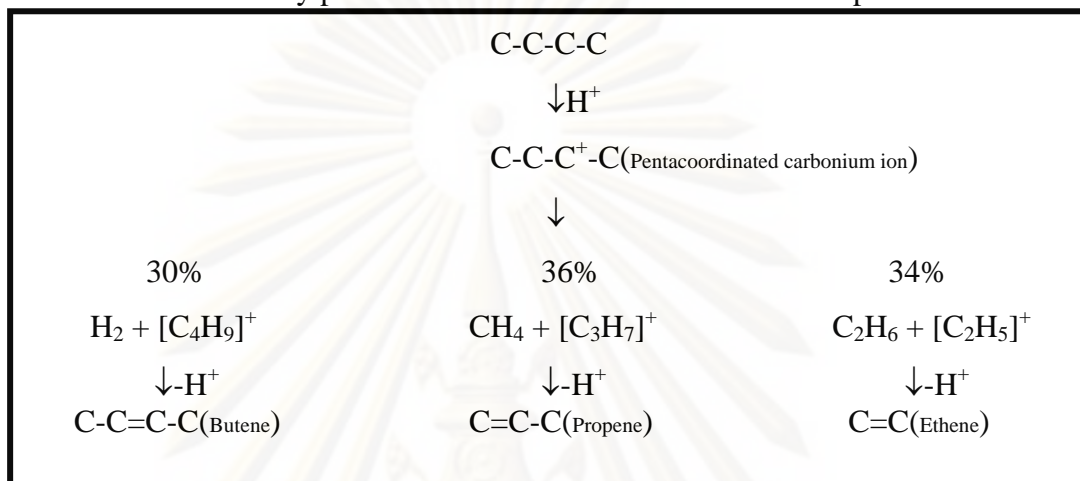


Figure 3.17 Propylene [<http://en.wikipedia.org/wiki/Propylene>]

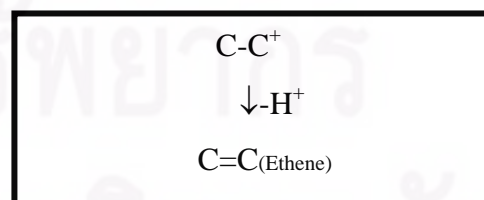
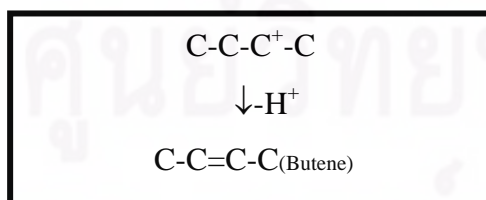
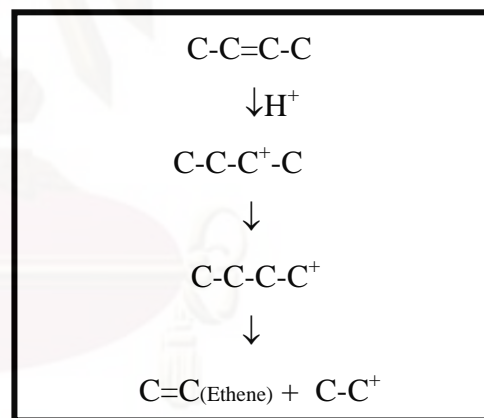
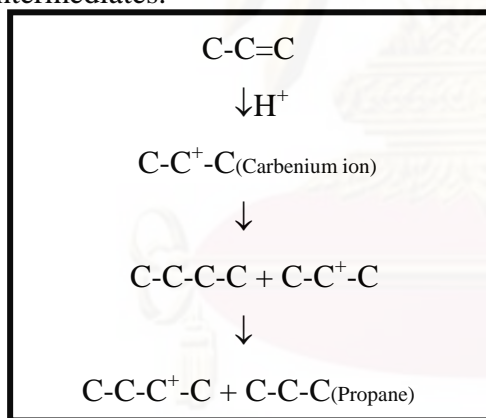
3.7 Reaction Mechanism of Butane to Ethylene and Propylene[17]

The results are consistent with the occurrence of two simultaneous mechanisms:

(1) A monomolecular mechanism proceeding through the pentacoordinated carbonium ion formed by protonation of the n-butane at the second position.



(2) A bimolecular hydride transfer proceeding through carbenium ion intermediates.



For isobutane mechanisms is same as n-butane.

CHAPTER IV

EXPERIMENTAL

4.1 Catalyst Preparation

In this study, having different Si/Al ratio (40, 70, 100) and two type of modified ZSM-5 catalysts (incipient impanation method and solid state ion exchange method) MgI/ZSM-5, MgS/ZSM-5, PI/ZSM-5 and PS/ZSM-5 were prepared for butane cracking. This catalyst used for selected the best catalyst for modified ZSM-5. The preparation of modified ZSM-5 were described as follows:

4.1.1 Chemicals

The details of chemicals used in the preparation procedure of ZSM-5 were shown in Table 4.1

Table 4.1 The chemicals used in the catalyst preparation

Chemical	Supplier
-Tetrapropyl ammonium bromide (TPABr)	Aldrich
-Sodium silicate solution (SiO ₂ 25.5-28.5%)	Merck
-Sodium hydroxide [NaOH]	Merck
-Aluminium chloride [AlCl ₃]	Aldrich
-Sulfuric acid [98.08%]	J.T.Baker
-Magnesium nitrate [Mg(NO ₃) ₂ .6H ₂ O]	BDH
-Ammonium hydro phosphate [(NH ₄) ₂ HPO ₄]	AR

4.1.2 Preparation of Na/ZSM-5

The preparation procedure of Na/ZSM-5 by rapid crystallization method was shown in Figure 4.1, while reagents were shown in table 4.2. This method can advantageously and rapidly prepare the uniform and fine zeolite crystals with the

following improvements: (i) the preparation of supernatant liquid was separated from that of gel, which was important to prepare the uniform crystals, (ii) the precipitated gel was milled before the hydrothermal treatment, which was essential to obtain the uniform and fine crystals, and (iii) the temperature under the hydrothermal treatment was programmed to minimize the time which was necessary for the crystallization. The detail preparation procedures of Na/ZSM-5 were described below.

Table 4.2 Reagents used for the preparation of Na/ZSM-5: Si/Al = 40

Solution for the gel preparation	Solution for the decant-solution preparation
<p><u>Solution A1</u></p> <p>AlCl₃ 1.125 g</p> <p>TPABr 5.72 g</p> <p>NaCl 11.95 g</p> <p>De-ionized water 60 ml</p> <p>H₂SO₄ 3.4 ml</p>	<p><u>Solution A2</u></p> <p>AlCl₃ 1.125 g</p> <p>TPABr 7.53 g</p> <p>De-ionized water 60 ml</p> <p>H₂SO₄ 3.4 ml</p>
<p><u>Solution B1</u></p> <p>De-ionized water 45 ml</p> <p>Sodium silicate 69 g</p>	<p><u>Solution B2</u></p> <p>De-ionized water 45 ml</p> <p>Sodium silicate 69 g</p>
<p><u>Solution C1</u></p> <p>TPABr 2.16 g</p> <p>NaCl 40.59 g</p> <p>NaOH 2.39 g</p> <p>De-ionized water 208 ml</p> <p>H₂SO₄ 1.55 ml</p>	<p><u>Solution C3</u></p> <p>NaCl 26.27 g</p> <p>De-ionized water 45 ml</p>

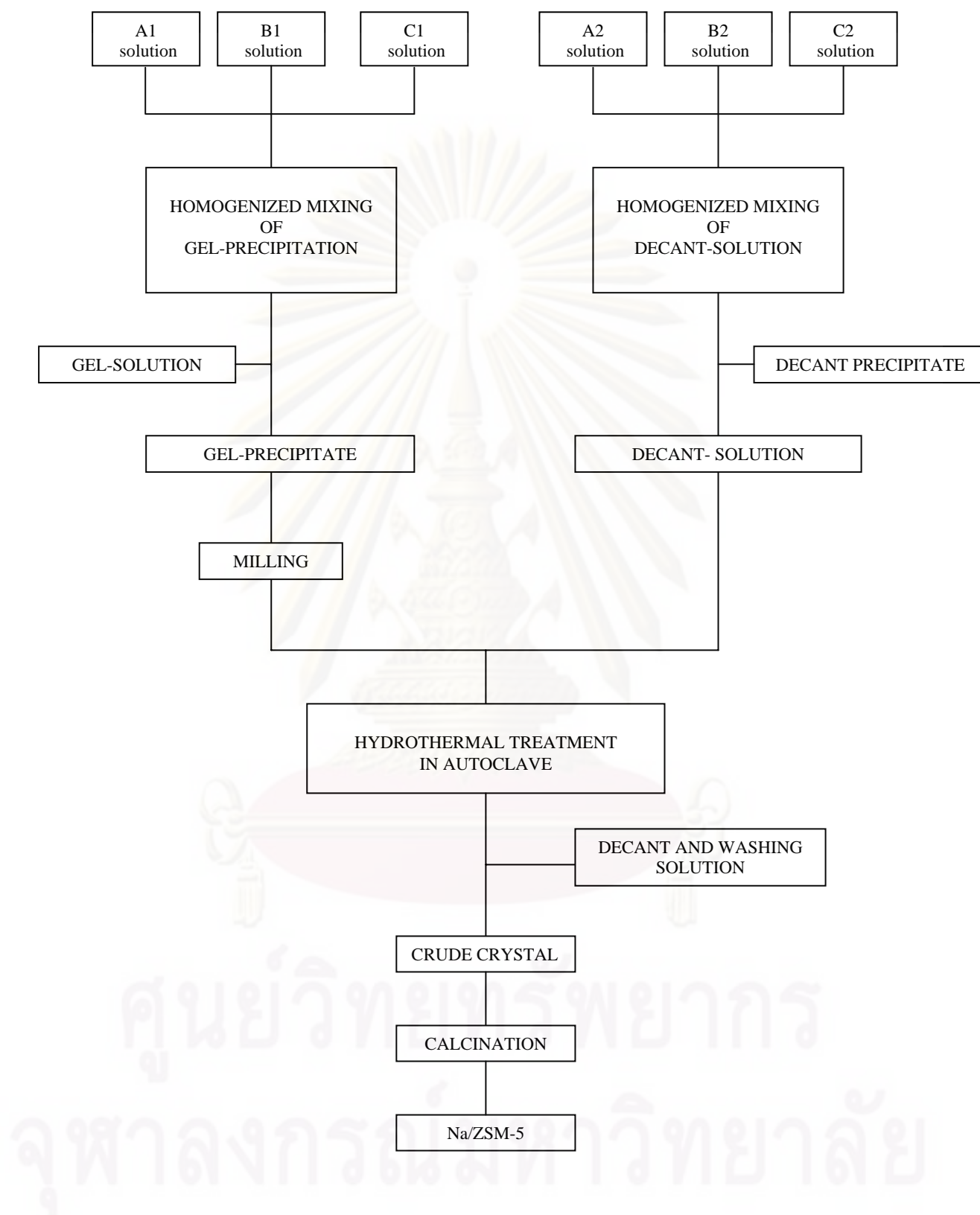


Figure 4.1 The preparation procedure of Na/ZSM-5 by rapid crystallization method.

4.1.2.1 Preparation of gel precipitation and decantation solution

A supernatant liquid was separated from the gel, which was important for preparing the uniform crystals. A gel mixture was prepared by adding solution A-1 and solution B-1 into solution C-1 drop wise with vigorous stirring using a magnetic stirrer at room temperature. The pH of the mixed solution was maintained within the range 9-11 because it was expected that this pH range was suitable for precipitation. The gel mixture was separated from the supernatant liquid by a centrifuge. The precipitated gel mixture was milled for 1 h by a powder miller (Yamato-Notto, UT-22). The milling procedure was as follows: milled 15 min → centrifuge (to remove the liquid out) → milled 15 min → centrifuge → milled 15 min. Milling the gel mixture before the hydrothermal treatment was essential to obtain the uniform, fine crystals.

A decantation solution was prepared by adding solution A-2 and solution B-2 into solution C-2 same as for the preparation of the gel mixture. During the time the supernatant liquid from A-2, B-2, and C-2 is mixing together. The pH of the solution was adjusted to between 9-11. H_2SO_4 (conc.) or 1 M NaOH solution were used to adjust pH of the decant mixture to an appropriate level if it is necessary. The colorless supernatant liquid was separated from the mixture by sedimentation and centrifugation.

4.1.2.2 Crystallization

The mixture of the milling precipitate and the supernatant of decant solution was charged in a 500 ml Pyrex glass container. The glass container was placed in a stainless steel autoclave. The atmosphere in the autoclave was replaced by nitrogen gas and pressurized up to 3 kg/cm^2 gauge. In order to vary the particle sizes of MFI, the mixture in the autoclave was heated from room temperature to 160 °C with various heating rates 0.4, 0.5, 0.9, 1.0, and 1.5 °C/min, and then up to 210 °C with a constant heating rate of 12 °C/h while being stirred at 60 rpm, followed by cooling of the hot mixture to room temperature in the autoclave overnight. The temperature was programmed to minimize the time necessary for the crystallization. The product

crystals were washed with de-ionized water about 8 times using the centrifugal separator (about 15-20 min. for each time), to remove Cl^- from the crystals, and dried in an oven at $110\text{ }^\circ\text{C}$ for at least 20 h.

4.1.2.3 Calcination

The dry crystals were calcined in an air stream at $540\text{ }^\circ\text{C}$ for 3.5 h, by heating them from room temperature to $540\text{ }^\circ\text{C}$ in 1 h, to burn off the organic template and leave the cavities and channels in the crystals. The calcined crystals were finally cooled to room temperature in a desiccator. The obtained Na/ZSM-5 was the parent Na/ZSM-5 which was further transformed to the other appropriate forms for the experiments in this study.

Moreover, Na/ZSM-5 obtained from each batch was checked by using the X-Ray Diffraction (XRD) analysis to confirm the ZSM-5 structure and crystallinity of sample. If, unfortunately, the XRD pattern could not be acceptable, the sample would be discarded and a new sample has to be made.

4.1.2.4 Ammonium ion-exchange

To make $\text{NH}_4/\text{ZSM-5}$, the parent Na/ZSM-5 powder was firstly mixed with 1 M NH_4NO_3 solution at 30 ml per gram of catalyst. In the procedure, the catalyst amounts did not exceed 5 grams to approach complete exchange. The slurry of zeolite and solution was then stirred and heated on a hot plate, maintained at $80\text{ }^\circ\text{C}$ by reflux. After heating the mixture for about 1 h, the mixture was cooled down to room temperature and centrifuged to remove the used solution. The remained crystals were mixed again with NH_4NO_3 solution in the same amount. The previous step was repeated. The exchanged catalyst was then washed twice with deionized water by using a centrifugal separator. Then, the ion exchange crystal was dried at $110\text{ }^\circ\text{C}$ for at least 3 h. in oven. The dried catalyst was obtained the NH_4 -form of ZSM-5. The $\text{NH}_4/\text{ZSM-5}$ was converted to H-form ZSM-5 by removing NH_3 species from the catalyst surface. NH_3 can be removed by thermal treatment of the $\text{NH}_4/\text{ZSM-5}$ zeolite. This was done by heating a sample in a furnace from ambient temperature to $540\text{ }^\circ\text{C}$

in 1 h and holding the sample at 540 °C for 3.5 h. After this step, the obtained crystals were H-zeolite.

4.1.3 Magnesium and phosphorus loading

4.1.3.1 Magnesium loading by incipient wetness impregnation method

MgI/HZSM-5 samples were prepared by impregnating the HZSM-5 zeolite with an aqueous solution of $\text{Mg}(\text{NO}_3)_2 \cdot 6\text{H}_2\text{O}$ by incipient wetness impregnation method. The impregnation period lasted for 6 hours in the temperature range of 30–40 °C and then dried at 120 °C and finally calcined at 327 °C in air atmosphere for 6 h.

4.1.3.2 Magnesium loading by solid state ion exchange method

MgS/ZSM-5 sample, HZSM-5 and magnesium nitrate in a given atomic ratio of Mg to lattice aluminium was carefully grinded in a mortar, calcined in an oven in static conditions at a heating rate of 10°C/min and at 327°C for 6 h, cooled, washed 5 times with deionised water, and finally dried overnight at 120°C.

4.1.3.3 Phosphorus loading by incipient wetness impregnation method

PI/HZSM-5 samples were prepared by impregnating the HZSM-5 zeolite with an aqueous solution of $(\text{NH}_4)_2\text{HPO}_4$ by incipient wetness impregnation method. The impregnation period lasted for 6 hours in the temperature range of 30–40 °C and then dried at 120 °C and finally calcined at 500 °C in air atmosphere for 4 h.

4.1.3.4 Phosphorus loading by solid state ion exchange method

PS/ZSM-5 sample, HZSM-5 and ammonium hydrogen phosphate in a given atomic ratio of P to lattice aluminium was carefully grinded in a mortar, calcined in an oven in static conditions at a heating rate of 10°C/min and at 500°C for 4 h, cooled, washed 5 times with deionised water, and finally dried overnight at 120°C.

4.2 Pretreatment Condition

The pretreatment procedure used in this study concerns the hydrothermal treatment condition. The catalysts were pretreated in N_2 while elevating the temperature from room temperature to reaction temperature in 1 h.

4.3 Characterization

4.3.1 X- Ray Diffraction analysis (XRD)

Crystallinity and X-ray diffraction (XRD) patterns of the catalysts were performed by a X-ray diffractometer SEIMENS D500 connected with a personal computer with Diffract AT version 3.3 program for fully control of the XRD analyzer. The experiments were carried out by using $CuK\alpha$ radiations with Ni filter and the operating condition of measurement are shown as follows:

2θ range of detection	:	4 – 40 °
Resolution	:	0.04 °
Number of Scan	:	10

The functions of based line subtraction and smoothing were used in order to get the well formed XRD spectra.

4.3.2 X-Ray Fluorescence analysis (XRF)

Quantities of SiO_2/Al_2O_3 in the sample were determined by atomic absorption spectroscopy using Varian, Spectra A8000 at the Department of Science Service, Ministry of Science Technology and Environment.

4.3.3 BET surface area measurement

The surface area (A_{BET}) of the samples was calculated using BET technique, Micromeritics ASAP 2020.

4.3.4 Scanning Electron Microscopy (SEM)

Scanning Electron Microscopy was employed for including the shape and size of the prepared zeolite crystal. The JEOL JSM-35 CF model at the Scientific and Technological Research Equipment Centre, Chulalongkorn University (STREC) was used for this purpose

4.3.5 Temperature Programmed Adsorptions of Ammonia (NH₃-TPD)

The acid properties were observed by Temperature programmed desorption (TPD) equipment by using micromeritics chemisorb 2750 Pulse Chemisorption System.

4.3.6 ²⁷Al Magnetic Angle Spinning Nuclear Magnetic Resonance (²⁷Al CP/MAS NMR)

Quantitative analysis of aluminum tetrahedral in zeolite was conformed by ²⁷Al – magnetic angle spinning nuclear magnetic resonance (Al CP/MAS NMR, BRUKER DPX-300 spectroscopy operating at 78 MHz) at National Metal and Materials Technology Center (MTEC) The signal of alumina tetrahedral could be detected at around 54 ppm. and the signal of alumina octrahedral could be detected at around 0 ppm.

4.4 Reaction Testing

4.4.1 Chemicals and reagents

Butane commercial (isobutane 1.2%, n-butane 1.15%, nitrogen balance) was available from TIG for butane cracking.

4.4.2 Instruments and apparatus

(a) Reactor: The reactor was a conventional micro reactor made from a stainless tube with 7 mm inside diameter. The reaction was carried out under N₂ gas flow and atmospheric pressure.

(b) Automatic Temperature Controller: This consists of a magnetic switch connected to a variable voltage transformer and a RKC temperature controller connected to a thermocouple attached to the catalyst bed in reactor. A dial setting established a set point at any temperatures within the range between 30°C to 700°C.

(c) Electric Furnace: This supply the required heated to the reactor for reaction. The reactor could be operated from room temperature up to 700° C at maximum voltage of 220 volt.

(d) Gas Controlling Systems: Nitrogen was equipped with pressure regulator (0-120 psig), an on-off valve and a needle valve were used to adjust flow rate of gas.

(e) Gas Chromatographs: Operating conditions were shown in Table 4.3.

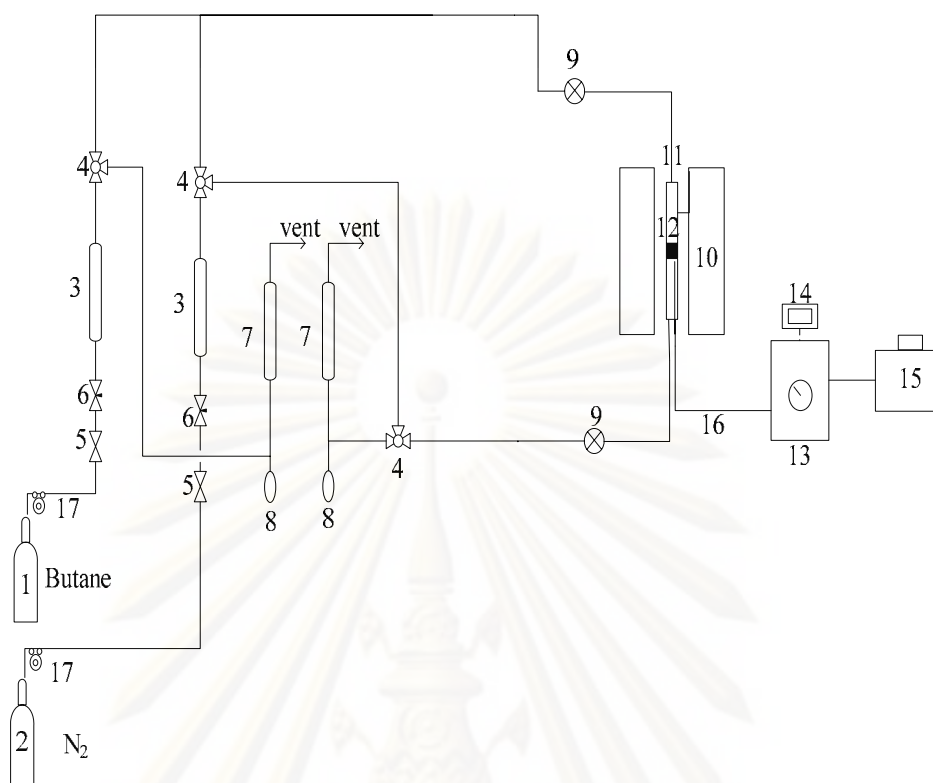
Table 4.3 Operating condition for gas chromatograph

Gas chromatograph	Shimadzu GC14B	Shimadzu GC14B
Detector	FID	FID
Column	VZ-10	Bentone 34
Carrier gas	N ₂ (99.999%)	He (99.999%)
Carrier gas flow	30 ml./min.	30 ml./min
Column temperature		
- Initial	75°C	100°C
Detector temperature	150°C	200°C
Injector temperature	100°C	200°C
Analyzed gas	Hydrocarbons(C1-C4)	Aromatics

4.4.3 Reaction method

The butane conversion was carried out by using a conventional flow as shown in Figure 4.2. A 0.1 portion of the catalyst was packed in the stainless tubular reactor. The reaction was carried out under the following procedure:

- 1) Adjust the pressure of nitrogen to 1 kg/cm^2 , and allow the gas to flow through a Rota meter, measure the outlet gas flow rate by using a bubble flow meter.
- 2) Heat up the reactor (under N_2 flow) by raising the temperature from room temperature to reaction temperature in 60 min and then hold at this temperature about 10 min for preheating catalyst.
- 3) Adjust the pressure of butane commercial (isobutane 1.2%, n-butane 1.15%, nitrogen balance) to 1 kg/cm^2 and allow the gas to flow through a Rota meter, measure the outlet gas flow rate by using a bubble flow meter.
- 4) Close nitrogen valve and open butane valve.
- 5) Start to run the reaction.
- 6) Take sample for analyzed by gas chromatograph after the reaction ran for 1 h.



- | | |
|----------------------------------|-----------------------------------|
| 1. Butane cylinder | 2. N ₂ cylinder |
| 3. Mass flow controller | 4. Three-way-valve |
| 5. Ball valve | 6. Needle valve |
| 7. Rotary meter | 8. Rubber cock |
| 9. Sampling point | 10. Furnace |
| 11. Reactor | 12. Catalyst bed |
| 13. Temperature controller | 14. Digital temperature indicator |
| 15. Variable voltage transformer | 16. Thermocouple/Thermometer |
| 17. Pressure regulator | |

Figure 4.2 Schematic diagram of the reaction apparatus for reaction.

CHAPTER V

RESULTS AND DISCUSSIONS

The chapter is divided into two sections. The first section involves the effect of reaction temperature and Si/Al ratios on butane to light olefins reaction. This section aims to select the suitable Si/Al ratios and temperature reaction to use in the second section. The second section focuses on the effect of modification method and metal loading on catalysts. Each section consisted of the catalyst characterization and catalytic reaction.

5.1 The Effect of Si/Al Ratio of ZSM-5 Catalyst and Reaction Temperature

5.1.1 Characterization of the catalyst

The commercial catalyst used in this work were first characterized in order to overview the difference of their characteristics and properties. The structure and crystallinity of MFI catalyst were measured by XRD. The specific surface area and amount of Si and Al in catalyst were measured to investigate their physical properties. The acidity of catalyst was measured by NH_3 -TPD

5.1.1.1 X-Ray Diffraction (XRD)

The X-Ray diffraction patterns for the commercial H/ZSM-5 of catalyst are shown in Figure 5.1. The X-Ray diffraction patterns for the catalyst prepared with various Si/Al ratios are illustrated in Figure 5.2. The patterns of catalyst prepared by the rapid crystallization method, were similar to those of H/ZSM-5. This indicated that all the prepared catalyst had the similar pentasil pore opening structure as H/ZSM-5.

5.1.1.2 Physical properties

The physical properties for all the catalysts are summarized in Table 5.1. The specific surface area estimated by BET and composition of catalyst in this study measured by XRF technique are also listed. The crystallinity was calculated based on the area of main peak of XRD compared with that of H/ZSM-5 as a reference. No significant loss of crystallinity was observed for all catalyst.

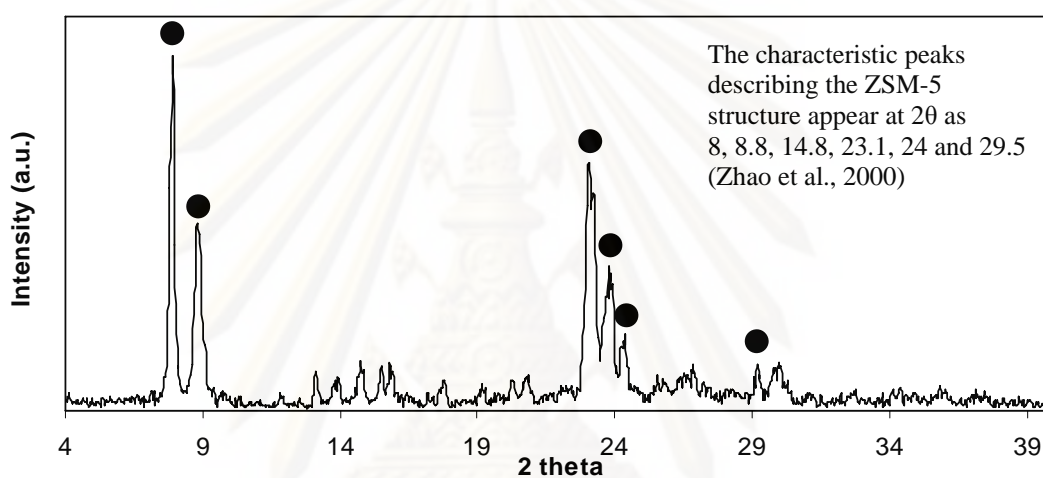


Figure 5.1 X-Ray diffraction pattern of commercial ZSM-5 zeolite

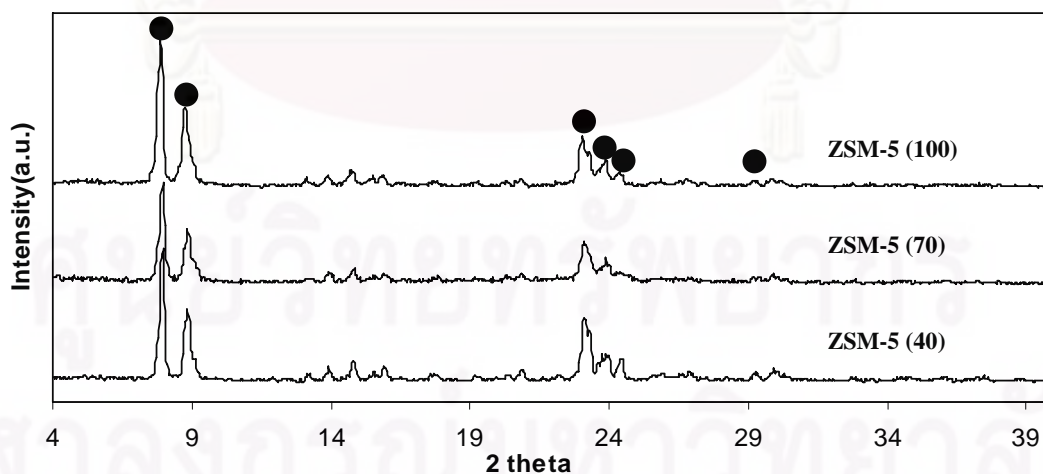


Figure 5.2 X-Ray diffraction patterns of H/ZSM-5 with various Si/Al ratios

Table 5.1 Physical properties of various Si/Al ratios of H/ZSM-5

Catalyst	Si/Al Ratio	Si/Al Ratio ^a Observed	BET Surface ^b Area (m ² /g)	Pore Volume (cm ³ /g) ^b	% Crystallinity ^c
H/ZSM-5	40	37.57	354	0.239	87.6
	70	69.92	363	0.244	85.5
	100	87.87	359	0.241	88.8

a measured by XRF, b based on N₂ physisorption (Multi-Point),
c based on XRD measurement

5.1.1.3 The acidity of catalyst

Table 5.2 shows the NH₃-TPD profiles of various Si/Al ratios. The profiles are composed of two peaks, i.e. a high temperature peak representing strong acid sites and a low temperature peak representing weak acid sites. It was found that high Si/Al ratio resulted in lower acidity than did the low Si/Al ratio. Figure 5.3 shows the NH₃-TPD profiles of various Si/Al ratios. The lower acidity of H/ZSM-5 (70) than that of H/ZSM-5 (100) may be attributed to less framework Al of H/ZSM-5 (70) than did H/ZSM-5 (100) as shown in Figure E.1

Table 5.2 Acidity of various Si/Al ratios of H/ZSM-5

Catalyst	Adsorbed Volume of Ammonia (ml)	Total Acid Site (mmol H ⁺ /g)
H/ZSM-5 (40)	12.5	4.8
H/ZSM-5 (70)	4.6	1.7
H/ZSM-5 (100)	8.8	3.1

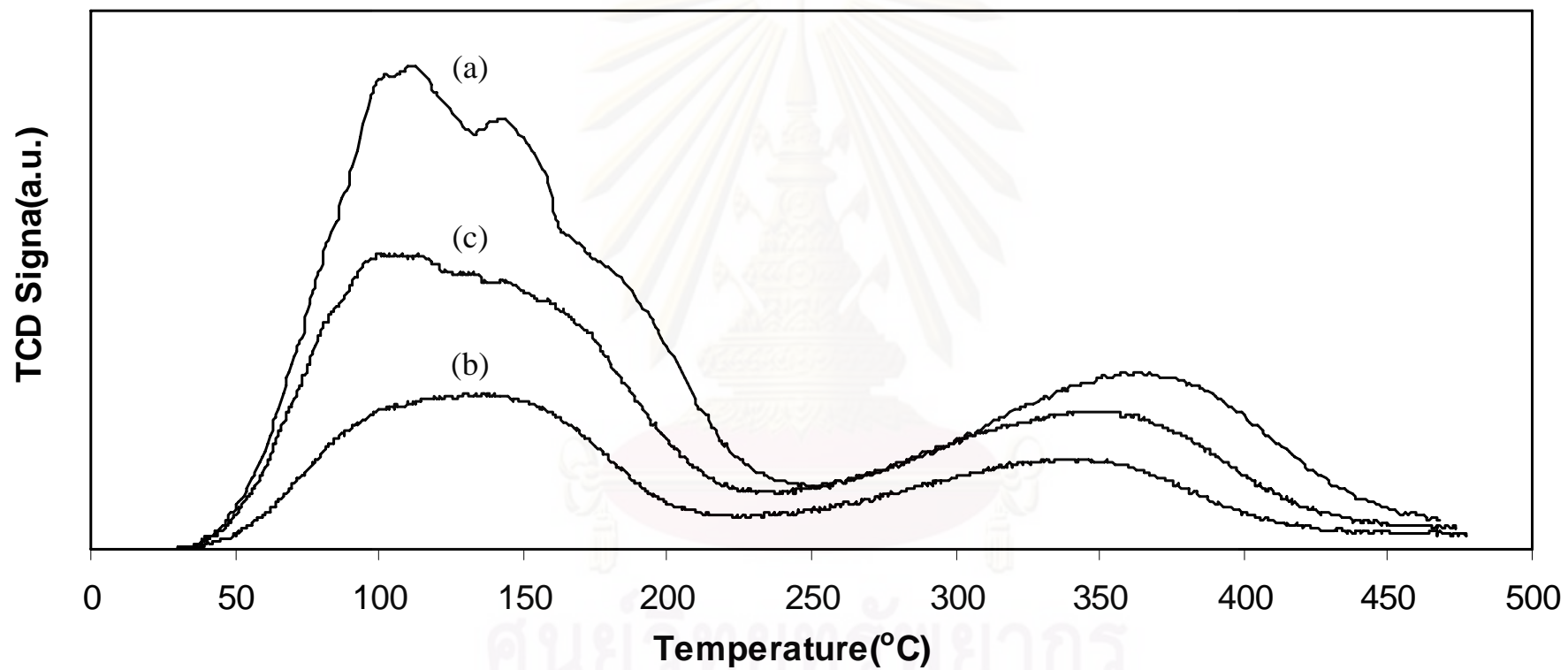


Figure 5.3 The NH_3 -TPD profiles of various Si/Al ratios of H/ZSM-5 catalysts.

(a) Si/Al = 40, (b) Si/Al = 70, (c) Si/Al = 100

5.1.2 Catalytic reaction

Figures 5.4-5.6 show the butane conversion and light olefins selectivity of butane cracking on H/ZSM-5 catalysts in various Si/Al ratios at the atmospheric pressure during the temperature range from 400 to 700°C. It has been revealed that at 400 °C, butane conversion did not occur, and then it increased rapidly from 450 °C up. The reaction temperature apparently affected butane conversion and light olefins selectivity. It was found that the suitable temperature to convert butane into light olefins was around 600 °C. In addition, the main products at high temperature were aromatic and paraffin.

The various Si/Al ratios of H/ZSM-5 catalyst were also studied. The butane conversion depends on Si/Al ratios of 40, 70 and 100. At 600 °C, Si/Al ratio of 70 low butane conversion because the catalyst having Si/Al ratio of 70 had lower acidity than the other Si/Al ratios. The light olefins selectivity of Si/Al of 70 was higher than other Si/Al ratios. The light olefins selectivity for Si/Al of 40 and 100 was also investigated at various reaction temperatures used in this study.

The results showed that the Si/Al ratio of H/ZSM-5 catalyst affected is responsible both butane conversion and light olefins selectivity where high acidity responded for the high butane conversion, but low light olefins selectivity was found

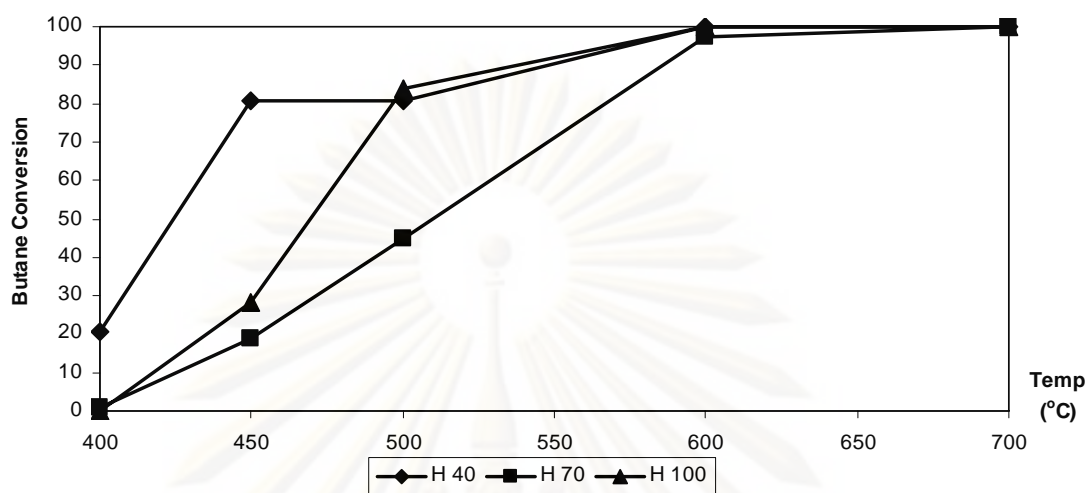


Figure 5.4 The effect of reaction temperature and Si/Al ratios of H/ZSM-5 catalysts on the butane conversion.

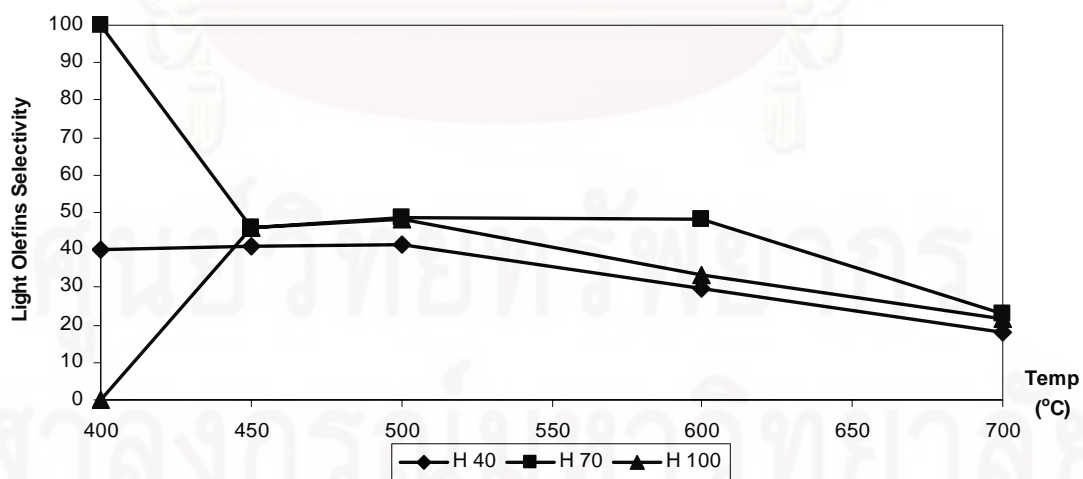


Figure 5.5 The effect of reaction temperature and Si/Al ratios of H/ZSM-5 catalysts on the light olefins selectivity.

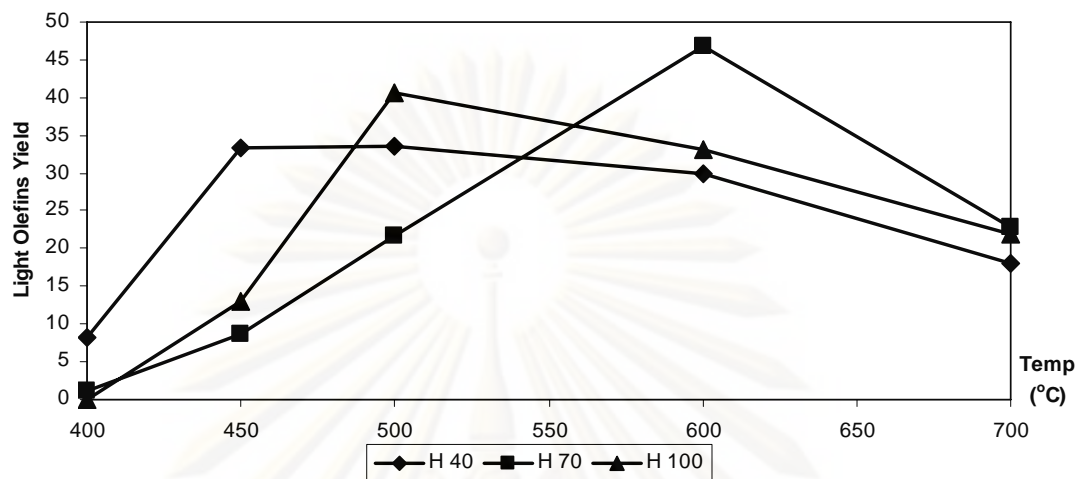


Figure 5.6 The effect of reaction temperature and Si/Al ratios of H/ZSM-5 catalysts on the light olefins yield.

Based on the light olefins yield obtained, it was found that the H/ZSM-5 at Si/Al ratio of 70 was the suitable catalyst at 600 °C that should be used for butane conversion to light olefins. Therefore, the Si/Al ratio of 70 and reaction temperature at 600 °C were selected for studying the effect of introduction method of phosphorus and/or magnesium to the catalysts, i.e. solid state ion exchange and incipient wetness impregnation, was studied.

5.2 The Effect of Methods, Phosphorus Loading and Magnesium Loading of Si/Al Ratio of ZSM-5 Catalyst

5.2.1 Characterization of the catalysts

The commercial catalyst used in this work was first characterized to overview the differences of their characteristics and properties. The structure and crystallinity of H/ZSM-5 catalyst were measured by XRD. The specific area and amount of Si and Al, methods, P and Mg catalyst were measured to investigate their physical properties. The morphology was determined by SEM. The acidity of catalyst was measured by NH₃-TPD.

5.2.1.1 X-Ray Diffraction pattern

The XRD patterns of P-modified H/ZSM-5 catalysts are shown in Figures 5.7 – 5.8. It has been shown that the XRD patterns of the samples obtained are almost typical to that of MFI topology. Neither peaks of impurities nor other significant change was observed for P-modified H/ZSM-5, though the relatively lower intensity was observed due to the decreasing crystallinity of P-modified samples obtained either by incipient wetness impregnation or solid state mixing. This indicates that the framework structure of H/ZSM-5 can be maintained even after modification with phosphorus.

On the other hand, The XRD patterns of Mg-modified H/ZSM-5 catalysts obtained either by incipient wetness impregnation or solid state mixing showed no significant decrease in crystallinity as shown in Figures. 5.9 – 5.10. It has been reported somewhere else[31] that some peak corresponding to MgO was observed around 2θ of 43° when the amount of Mg loading was 10 %wt or higher. Since the Mg loading amount in Mg- modified samples here were much lower than 10 %wt, thus, no formation of MgO phase has been expected.

No significant change of ZSM-5 structure was observed for various modification.

5.2.1.2 Morphology

Images for the Scanning electron microscopy (SEM) of the prepared catalysts are shown in Figures 5.11 – 5.14. The shapes of all catalyst are crystallize grouping but in Figures 5.15 – 5.18. The shapes of all catalyst are crystallize individuality.



ศูนย์วิทยทรัพยากร
จุฬาลงกรณ์มหาวิทยาลัย

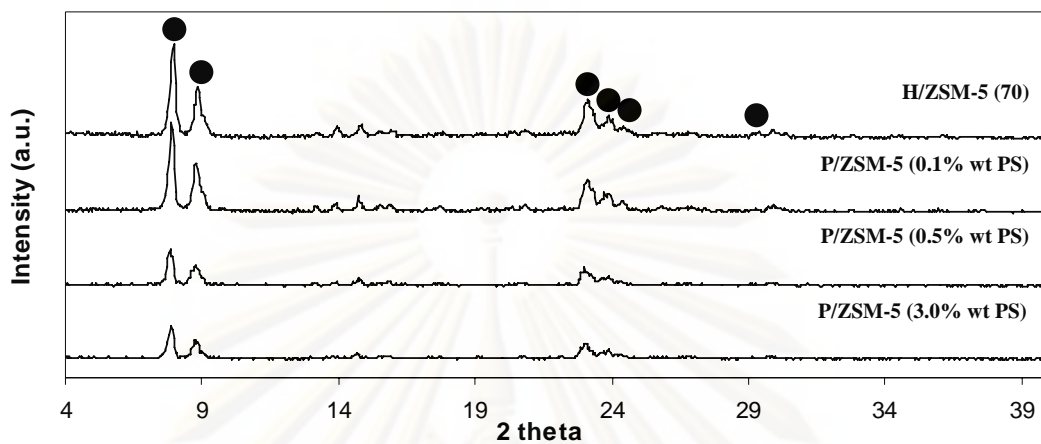


Figure 5.7 X-Ray diffraction patterns of P/ZSM-5 catalysts in the solid state ion exchange method.

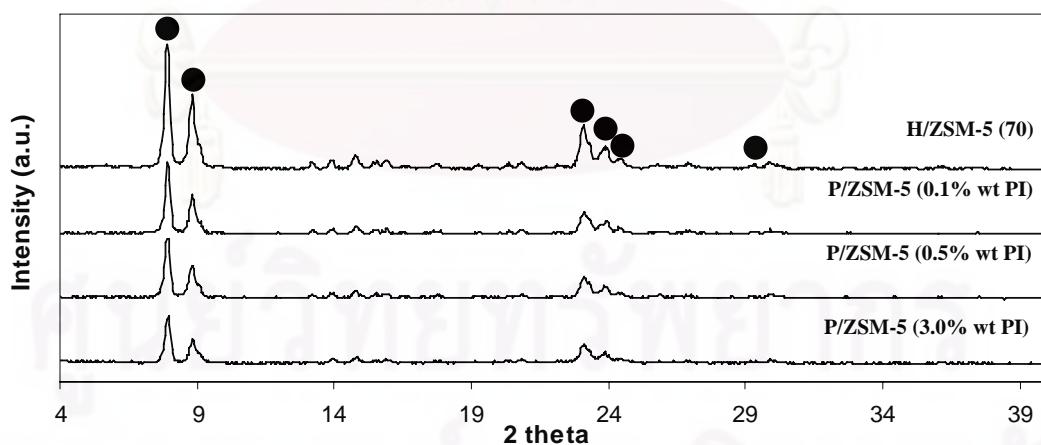


Figure 5.8 X-Ray diffraction patterns of P/ZSM-5 catalysts in the incipient wetness impregnation method.

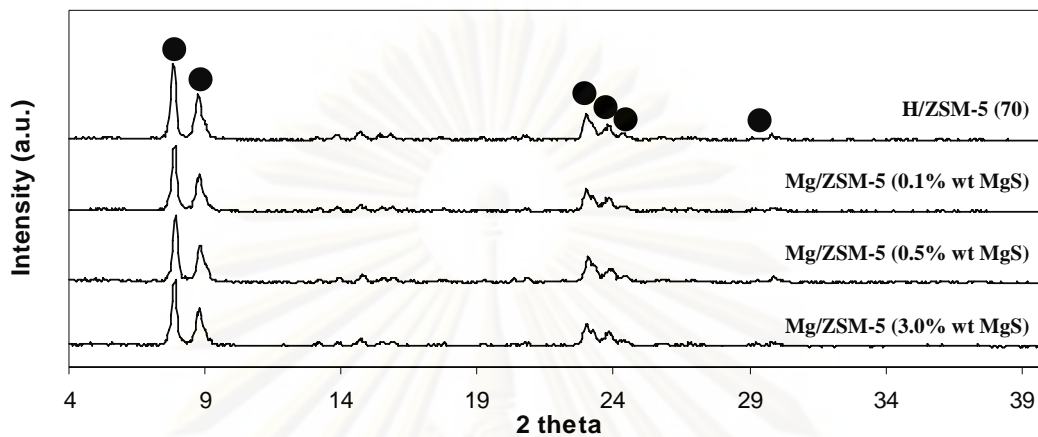


Figure 5.9 X-Ray diffraction patterns of Mg/ZSM-5 catalysts in the solid state ion exchange method.

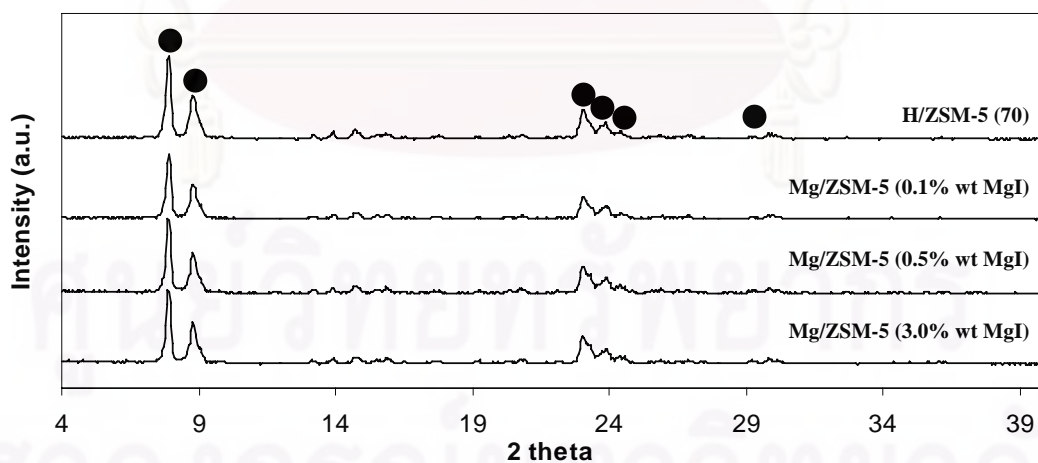


Figure 5.10 X-Ray diffraction patterns of Mg/ZSM-5 catalysts in the incipient wetness impregnation method.

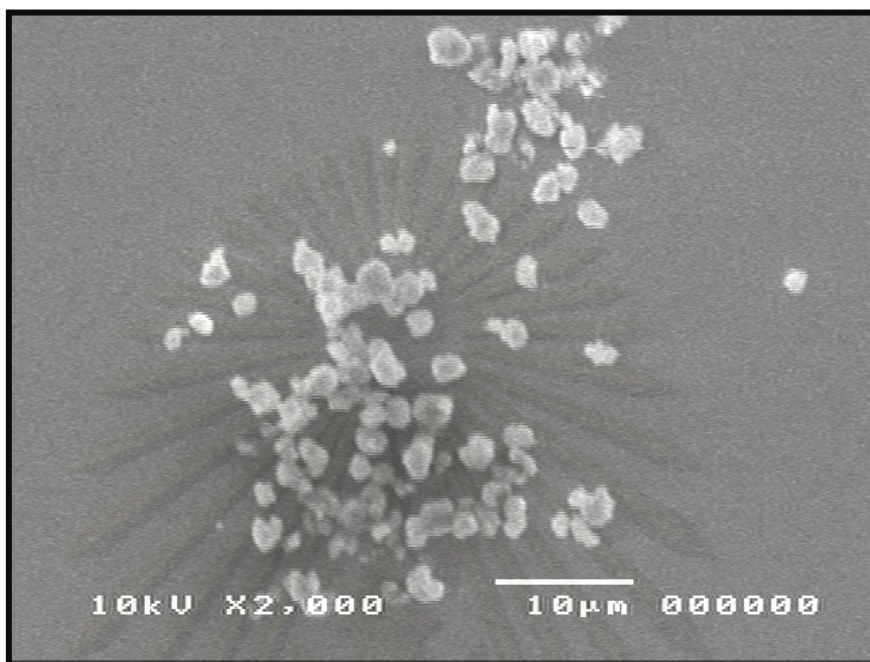


Figure 5.11 Scanning electron micrograph of P/ZSM-5 (0.1% wt PS)x 2000

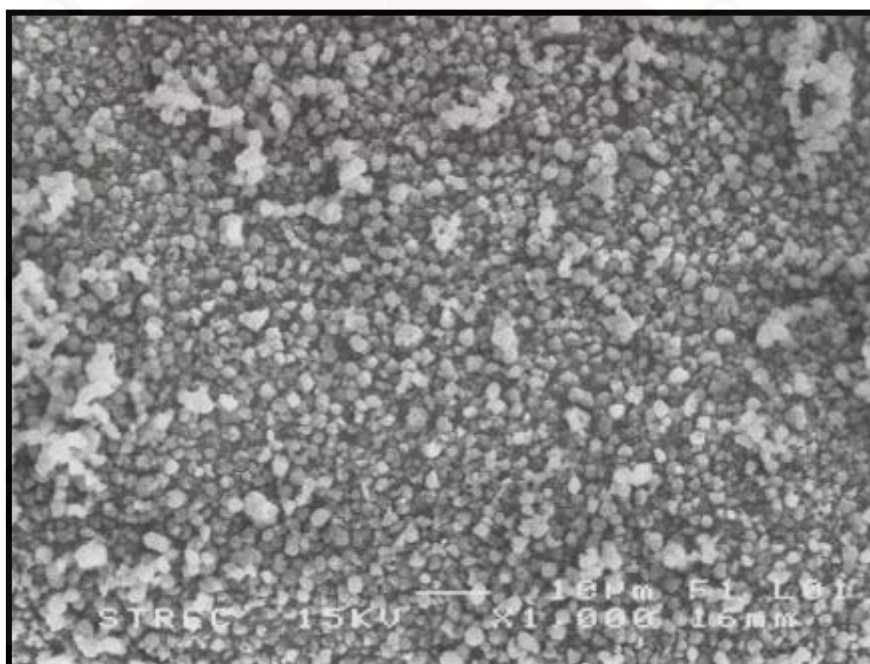


Figure 5.12 Scanning electron micrograph of P/ZSM-5 (0.1% wt PS)x 1000

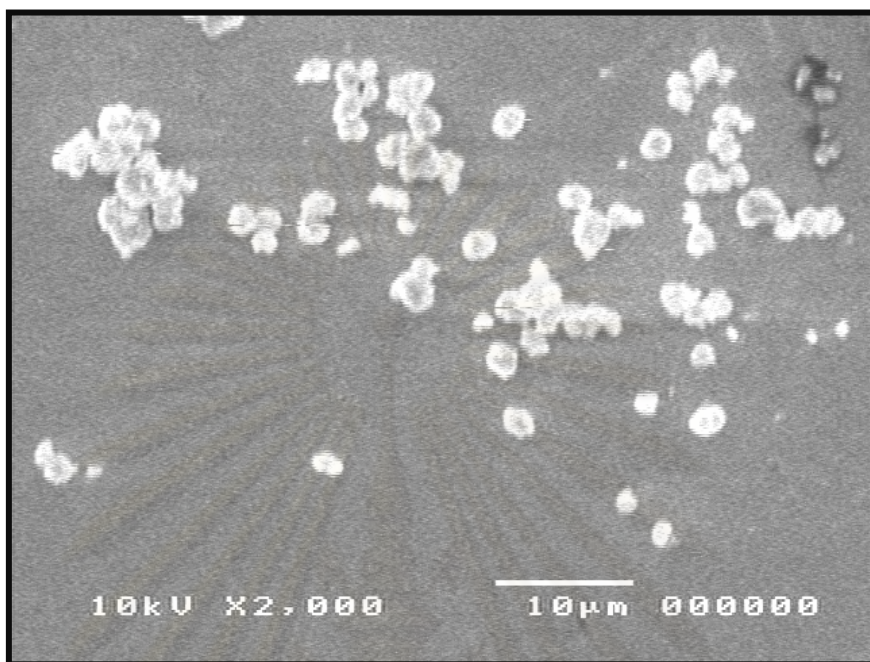


Figure 5.13 Scanning electron micrograph of P/ZSM-5 (0.1% wt PI)x 2000

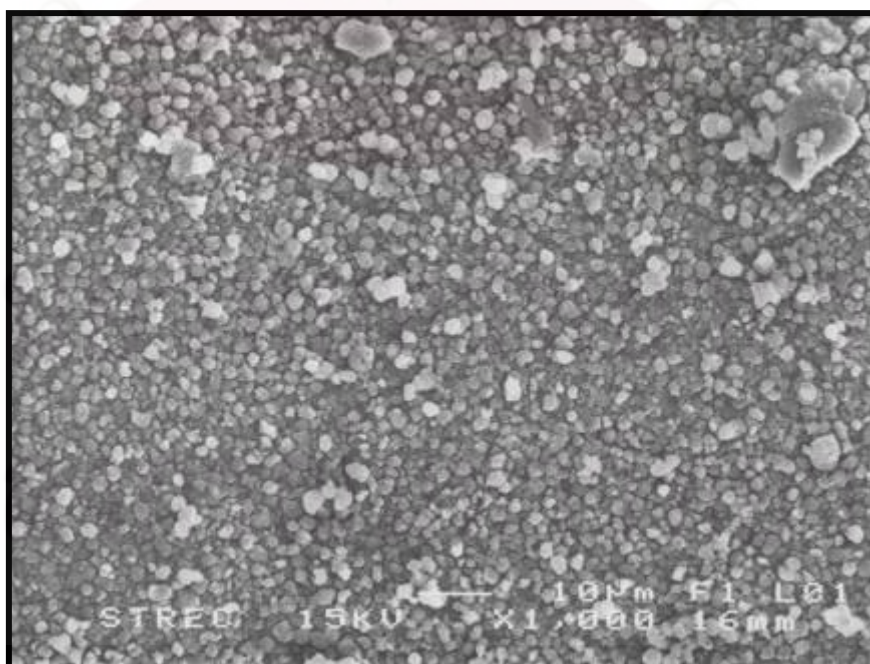


Figure 5.14 Scanning electron micrograph of P/ZSM-5 (0.1% wt PI)x 1000

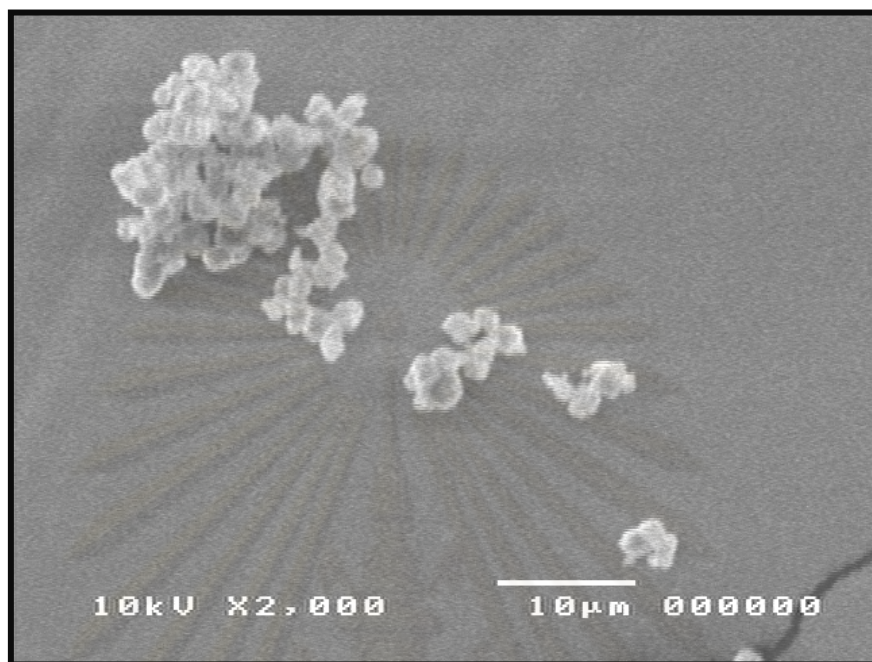


Figure 5.15 Scanning electron micrograph of Mg/ZSM-5(0.1% wt MgS)x 2000

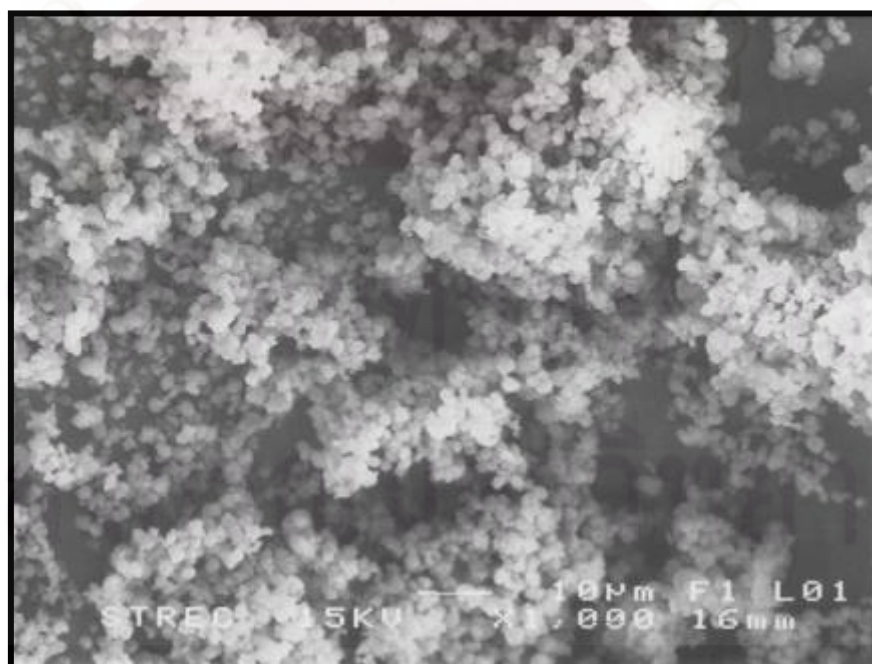


Figure 5.16 Scanning electron micrograph of Mg/ZSM-5 (0.1% wt MgS)x 1000

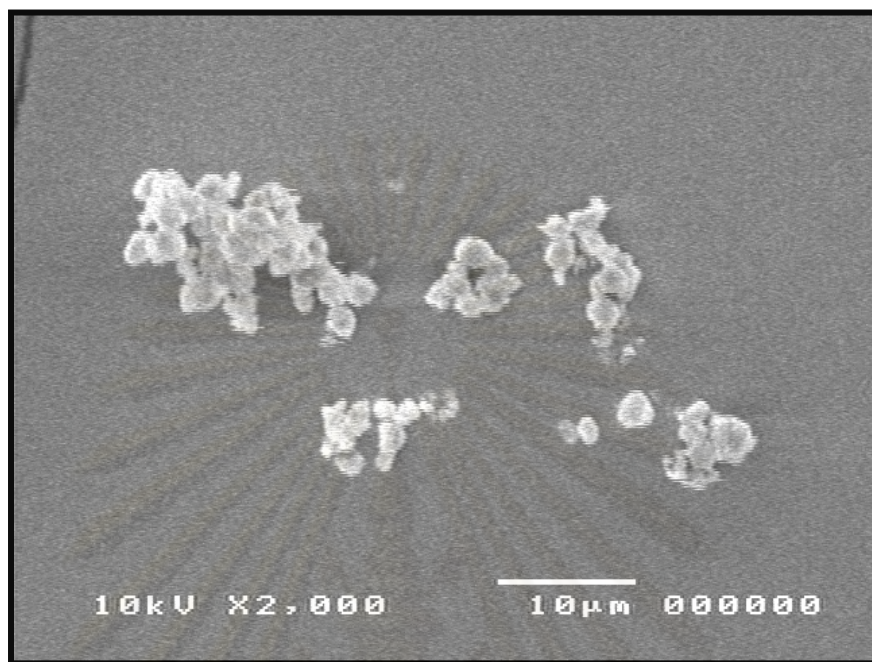


Figure 5.17 Scanning electron micrograph of Mg/ZSM-5 (0.5% wt MgI)x 2000

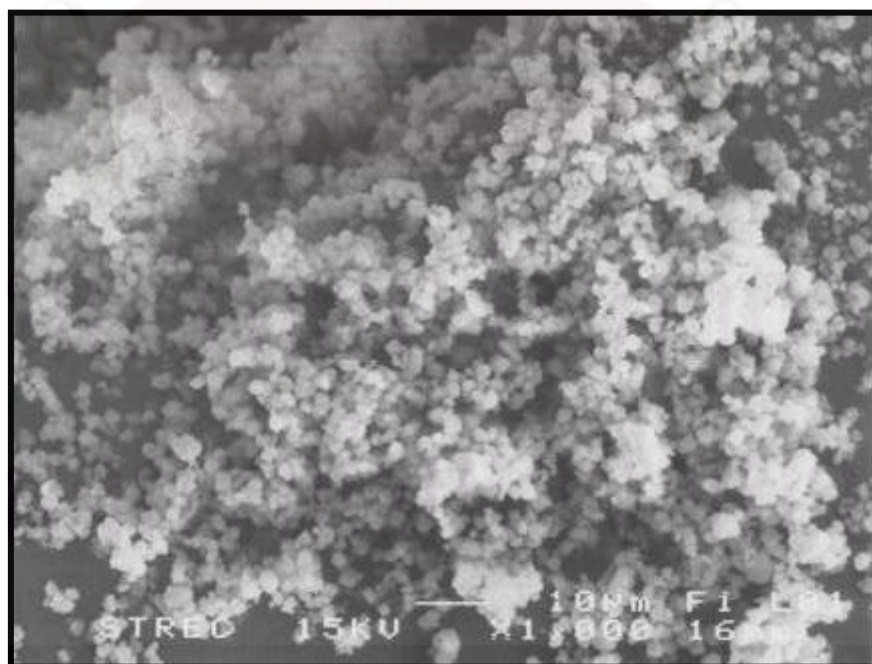


Figure 5.18 Scanning electron micrograph of Mg/ZSM-5 (0.5% wt MgI)x 1000

5.2.1.3 Physical properties

In Table 5.3, BET surface area decreased after the phosphorus and magnesium loading in ZSM-5 indicates same pore blocking by magnesium species and phosphorus species, especially magnesium species may be either dispersed in the channels or deposited at the other surface of the zeolite. Table 5.3 shows the zeolite catalysts with Si/Al ratio of 70 vary with methods, phosphorus content and magnesium content. Crystallinity, as determined by XRD, was calculated based on the area of main peak compare with the commercial ZSM-5 as a reference. The crystallinities of phosphorus loading decreased but the crystallinities of magnesium loading are the same.

Table 5.3 Physical properties of various methods and species of H/ZSM-5 catalyst

Catalyst	BET Surface Area (m ² /g)	Pore Volume(cm ³ /g)	%Crystallinity
H/ZSM-5	363	0.244	85.5
PS 0.1%	335	0.230	84.7
PS 0.5%	313	0.221	57.2
PS 3.0%	302	0.215	45.3
PI 0.1%	352	0.240	69.7
PI 0.5%	337	0.232	48.1
PI 3.0%	311	0.218	41.5
MgS 0.1%	183	0.155	83.0
MgS 0.5%	175	0.149	82.5
MgS 3.0%	153	0.138	81.7
MgI 0.1%	221	0.175	82.7
MgI 0.5%	194	0.161	83.1
MgI 3.0%	171	0.149	82.9

5.2.1.4 Acidity

The NH₃-TPD profiles of PS/ZSM-5, PI/ZSM-5, MgS/ZSM-5 and MgI/ZSM-5 catalyst are shown in Table 5.4. The profiles are composed of two peaks, i.e., a high temperature peak represents strong acid sites and a low temperature peak refers to weak acid sites (Inui, T., 1984)

From the Figures 5.19 – 5.22, they show NH₃-TPD profiles of various %wt phosphorus loading, magnesium loading and the methods. The NH₃-TPD profiles revealed loss of strong acid site after loading species.

Table 5.4 The peak concentration of acid site of the various methods and species of ZSM-5 catalyst

Catalyst	Adsorbed Volume of Ammonia (ml)	Total Acid Site (mmol H ⁺ /g)	Weak/Strong Acid Site
P/ZSM-5 (0.1% wt PS)	9.1	3.6	1.758
P/ZSM-5 (0.5% wt PS)	7.4	3.0	1.893
P/ZSM-5 (3.0% wt PS)	7.4	2.8	2.297
P/ZSM-5 (0.1% wt PI)	8.9	3.5	1.789
P/ZSM-5 (0.5% wt PI)	8.5	3.2	1.909
P/ZSM-5 (3.0% wt PI)	7.5	3.1	2.332
Mg/ZSM-5 (0.1% wt MgS)	9.4	3.7	1.428
Mg/ZSM-5 (0.5% wt MgS)	6.7	2.8	1.546
Mg/ZSM-5 (3.0% wt MgS)	6.1	2.3	1.911
Mg/ZSM-5 (0.1% wt MgI)	12.0	4.5	1.113
Mg/ZSM-5 (0.5% wt MgI)	10.8	4.3	1.405
Mg/ZSM-5 (3.0% wt MgI)	9.4	3.8	1.824

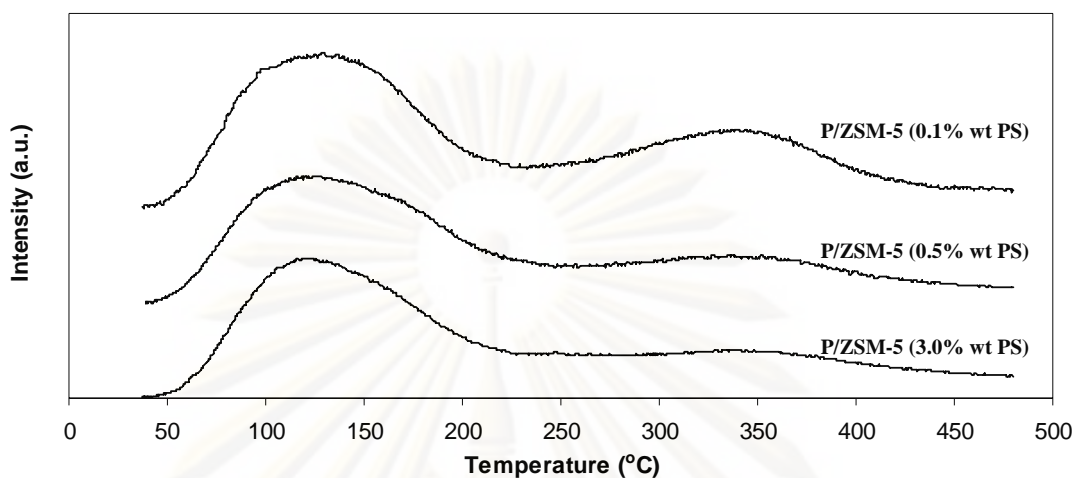


Figure 5.19 The NH₃-TPD profiles of P/ZSM-5 catalysts on various loading in the solid state ion exchange method.

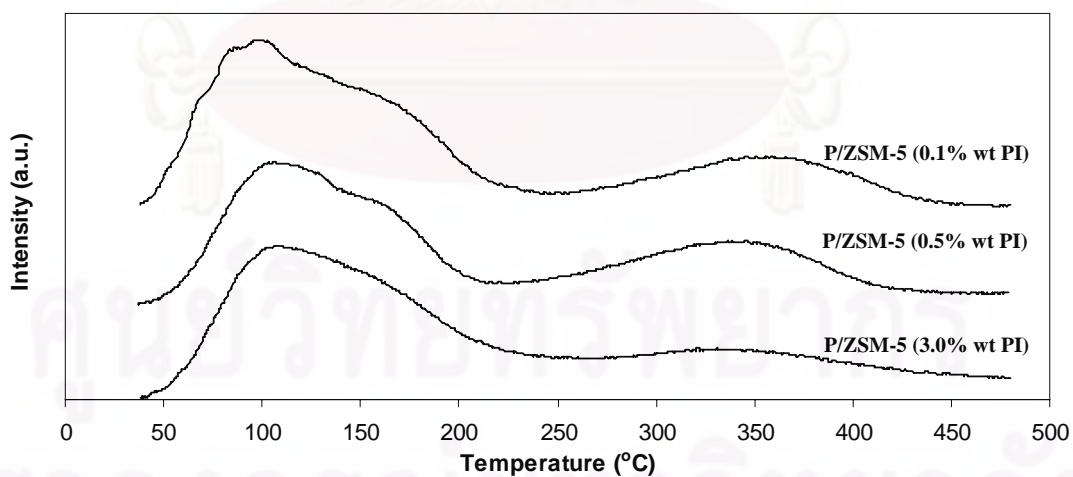


Figure 5.20 The NH₃-TPD profiles of P/ZSM-5 catalysts on various loading in the incipient wetness impregnation method.

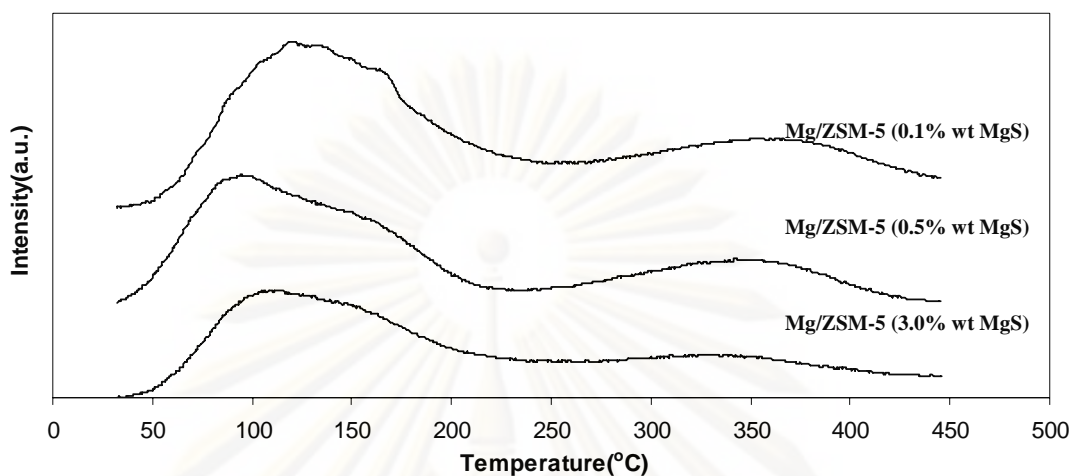


Figure 5.21 The NH₃-TPD profiles of Mg/ZSM-5 catalysts on various loading in the solid state ion exchange method.

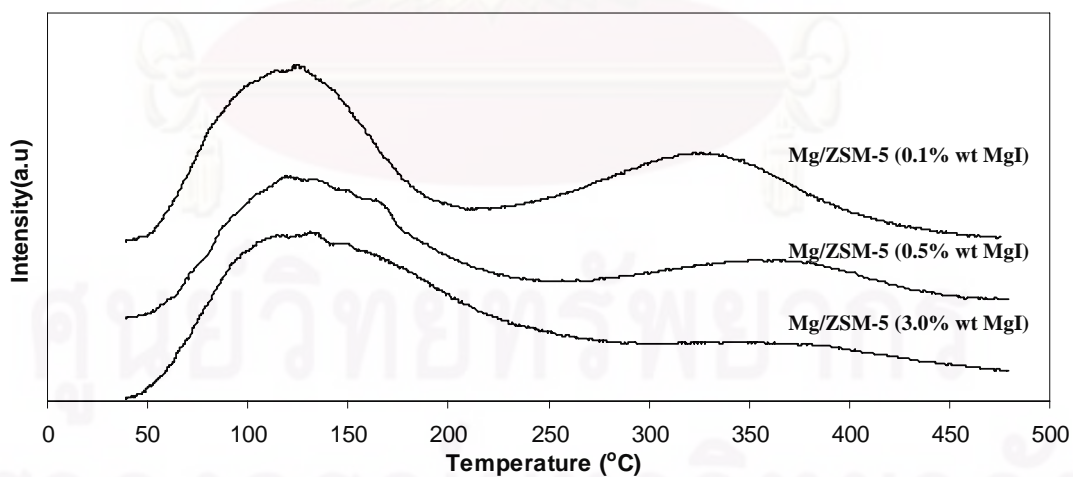


Figure 5.22 The NH₃-TPD profiles of Mg/ZSM-5 catalysts on various loading in the incipient wetness impregnation method.

5.2.2 Catalytic reaction

In this section, the catalytic properties of the catalysts prepared in this research are investigated by testing the butane conversion into light olefins (isobutane 1.2%, n-butane 1.15%, nitrogen balance)

The effect of loading methods

The effect of loading methods on the light olefins yield was compared. The modification methods of ZSM-5 (solid state ion exchange and incipient wetness impregnation) showed indifference on the light olefins yield. As shown in Figure 5.23 – 5.28

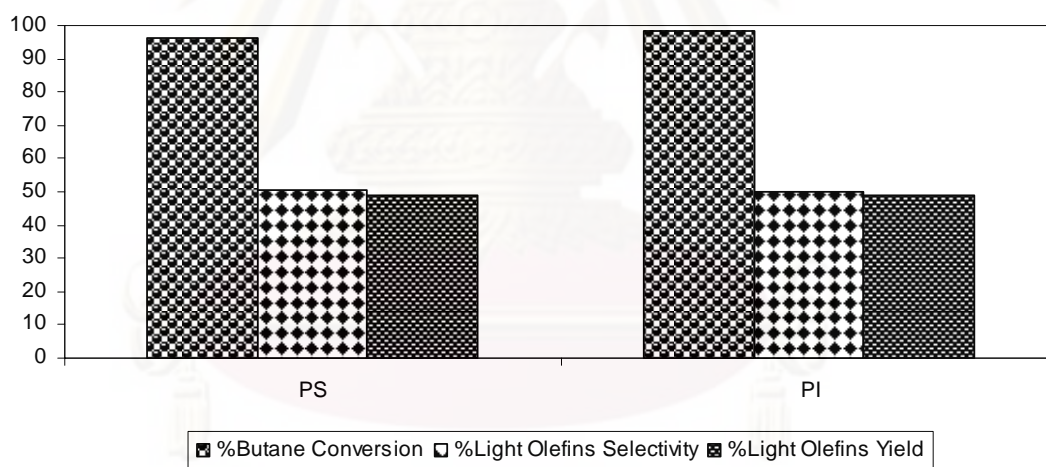


Figure 5.23 The effect of methods of P/ZSM-5 on butane conversion and light olefins selectivity in 0.1% wt.

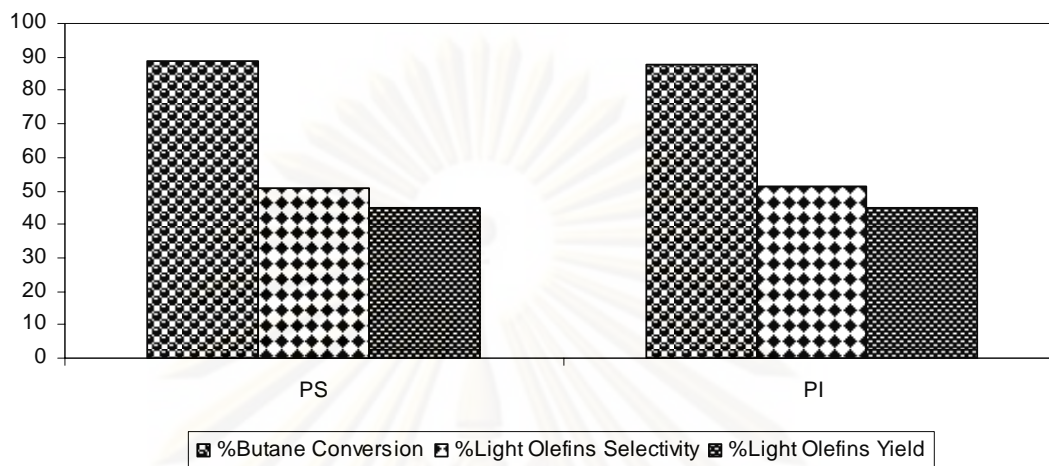


Figure 5.24 The effect of methods of P/ZSM-5 on butane conversion and light olefins selectivity in 0.5% wt.

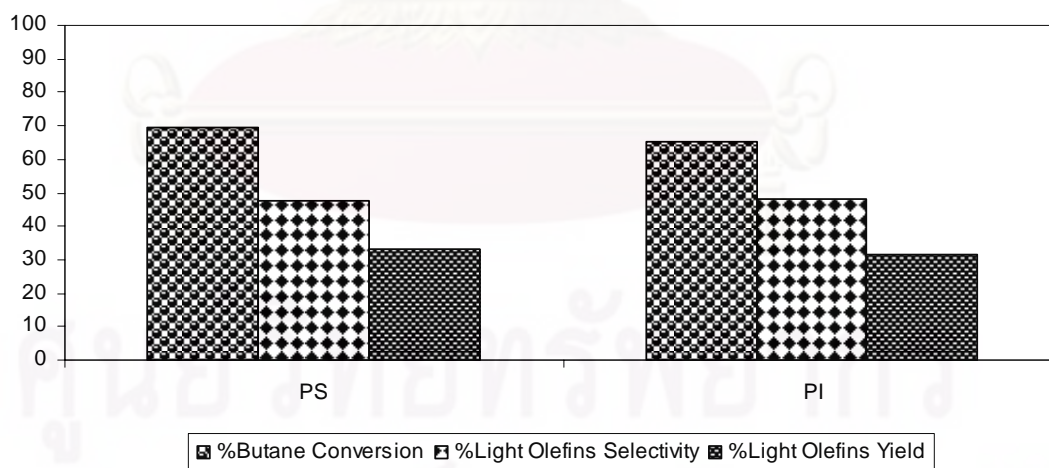


Figure 5.25 The effect of methods of P/ZSM-5 on butane conversion and light olefins selectivity in 3.0% wt.

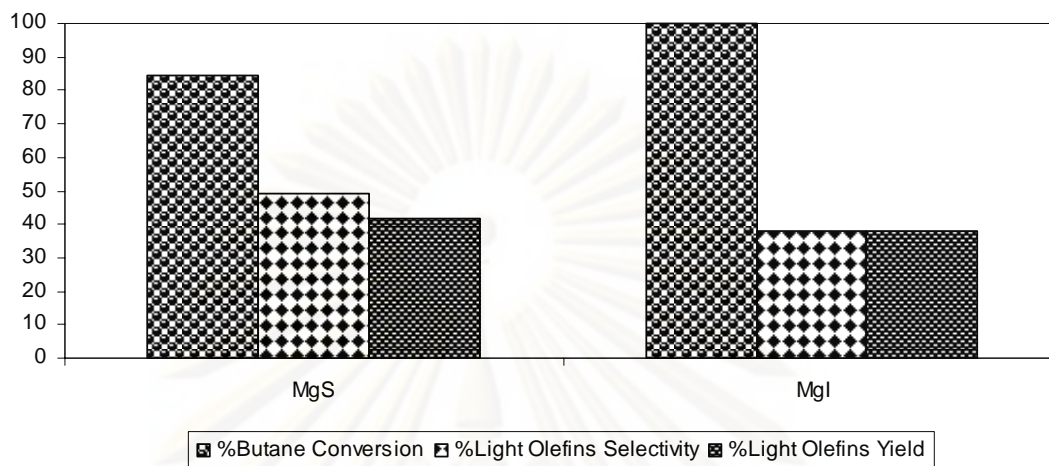


Figure 5.26 The effect of methods of Mg/ZSM-5 on butane conversion and light olefins selectivity in 0.1% wt.

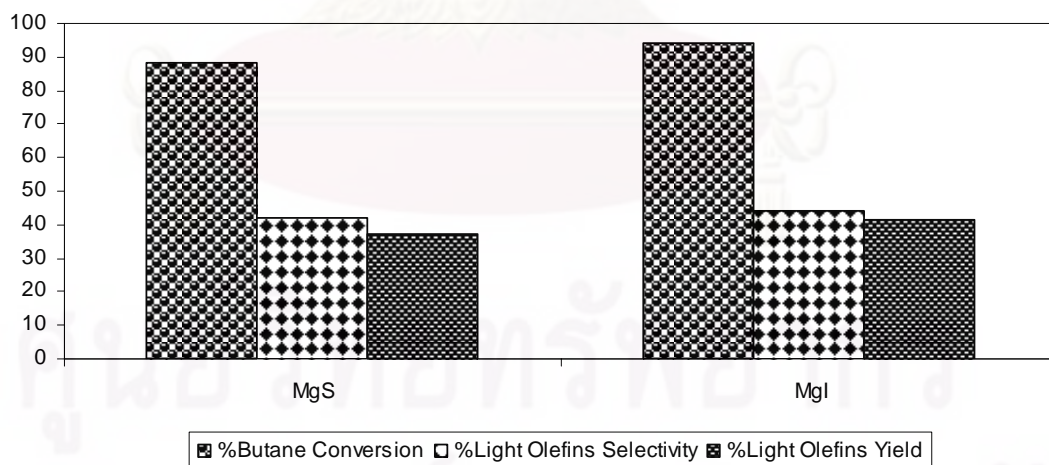


Figure 5.27 The effect of methods of Mg/ZSM-5 on butane conversion and light olefins selectivity in 0.5% wt.

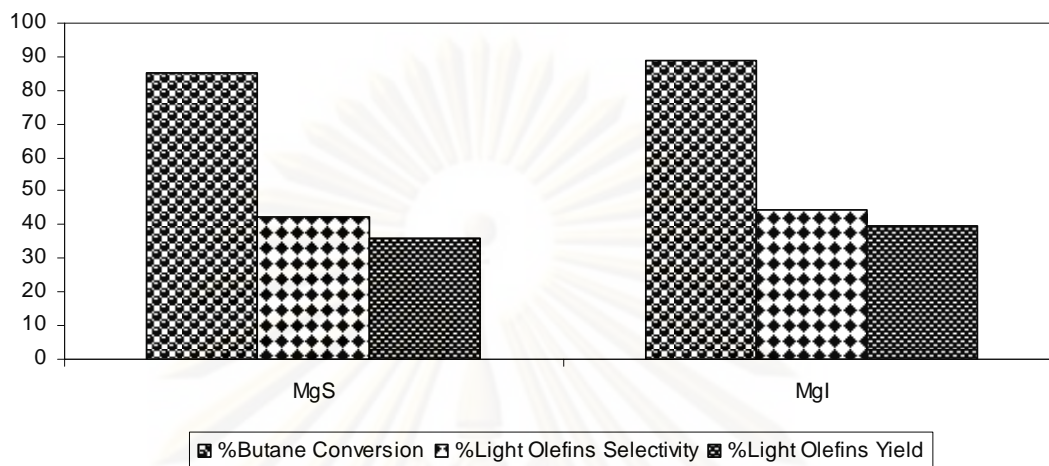


Figure 5.28 The effect of methods of Mg/ZSM-5 on butane conversion and light olefins selectivity in 3.0% wt.

The effect of species on the butane conversion

The effect of species on the butane conversion was compared. In phosphorus loading, the butane conversion decreases maybe by crystallinity that decrease when load phosphorus. In magnesium loading, the butane conversion decrease maybe by pore blocking.

The effect of species on the light olefins selectivity

The effect of species on the light olefins selectivity was compared. In the solid state ion exchange method, the light olefins selectivity of the phosphorus loading was maximum in 0.1% that same as magnesium loading. But in the incipient wetness impregnation method, the light olefins selectivity of the phosphorus loading was maximum in 0.5% that same as magnesium loading. As shown in Figure 5.29 – 5.33

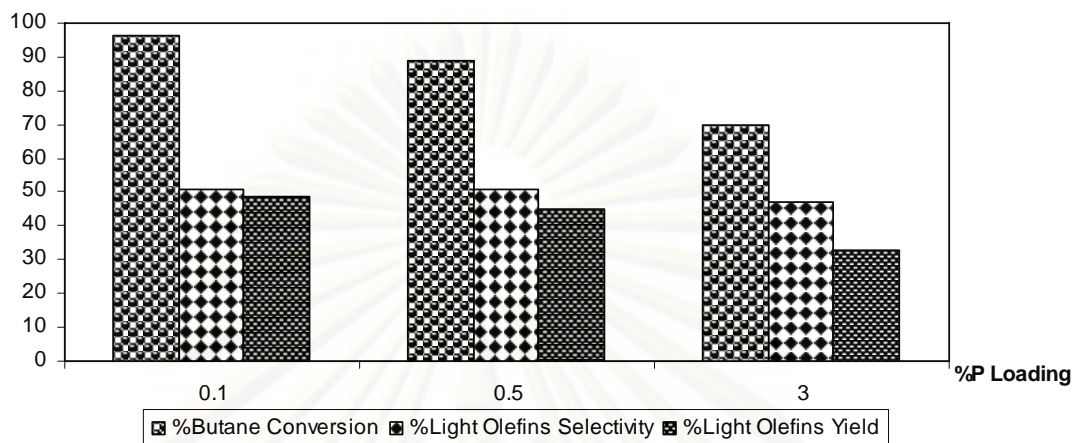


Figure 5.29 The effect of species of P/ZSM-5 on butane conversion and light olefins selectivity in the solid state ion exchange method.

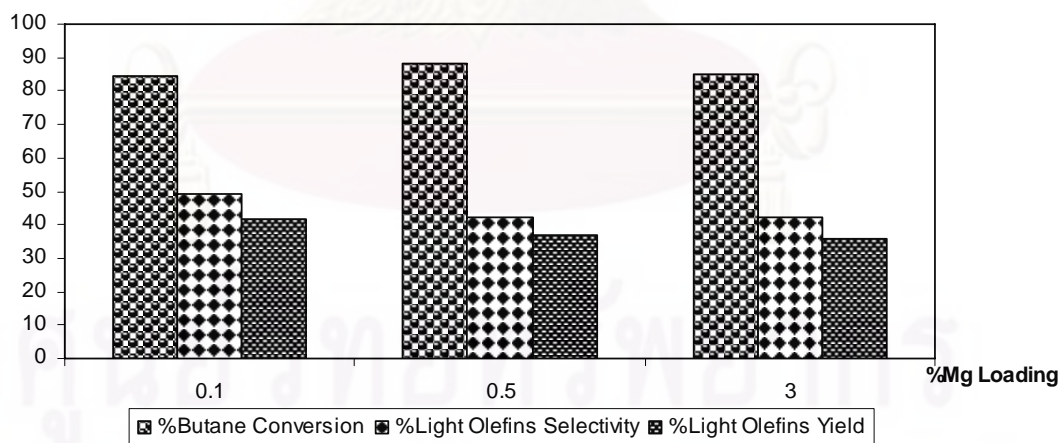


Figure 5.30 The effect of species of Mg/ZSM-5 on butane conversion and light olefins selectivity in the solid state ion exchange method.

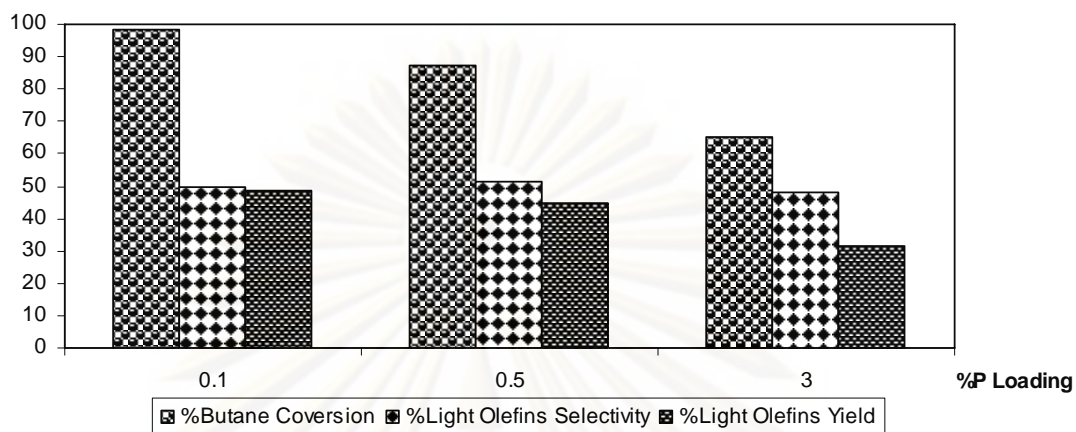


Figure 5.31 The effect of species of P/ZSM-5 on butane conversion and light olefins selectivity in the incipient wetness impregnation method.

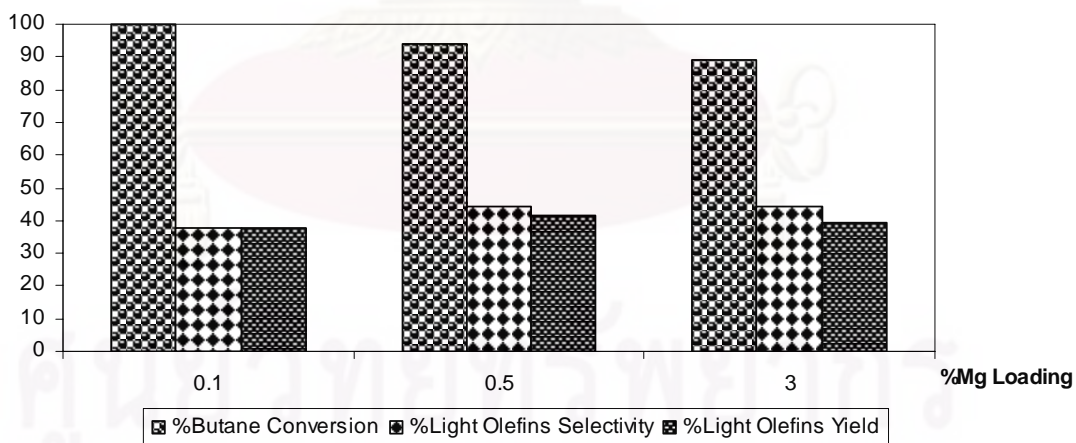


Figure 5.32 The effect of species of Mg/ZSM-5 on butane conversion and light olefins selectivity in the incipient wetness impregnation method.

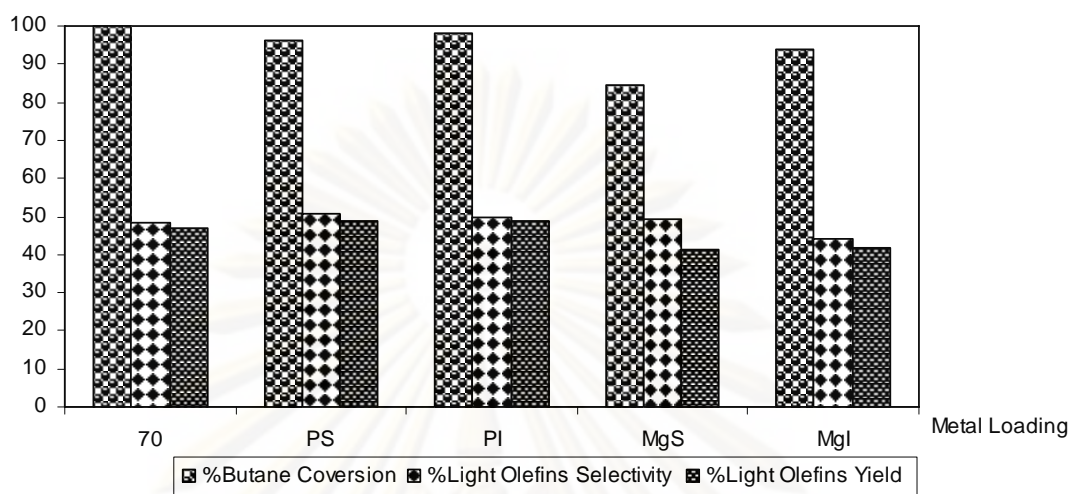


Figure 5.33 The effect of species of modified ZSM-5 on butane conversion and light olefins selectivity.

CHAPTER VI

CONCLUSIONS AND RECOMMENDATIONS

6.1 Conclusions

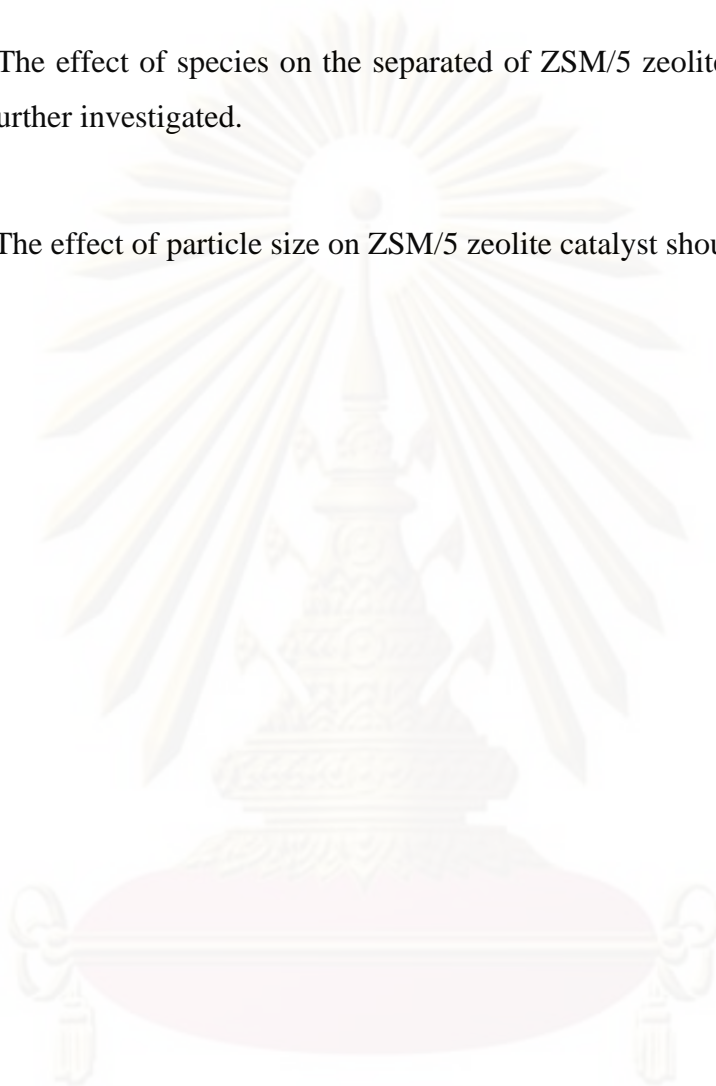
In this thesis, the several effect of ZSM-5 and modified ZSM-5 catalyst were tested for butane conversion into light olefin. The conclusions of this research were summarized as following:

1. The Si/Al ratios of H/ZSM-5 catalysts affected the butane conversion and light olefins selectivity. Higher acidity resulted in high butane conversion but low light olefin selectivity.
2. Based on the light olefins yield, it was found that the H/ZSM-5 with Si/Al of 70 was suitable catalyst at the reaction temperature 600 °C for butane conversion to light olefins.
3. The modification methods of ZSM-5 (solid state ion exchange and incipient wetness impregnation) showed indifference on the light olefins yield.
4. The light olefins yield in phosphorus-modified ZSM-5 was higher than that of magnesium-modified ZSM-5 one.
5. The butane conversion decreased with the introduction of phosphorus and/or magnesium into the H/ZSM-5 catalyst indicating an alteration of the parent zeolite, probably because of pore blocking in magnesium species and crystallinity in phosphorus species.
6. The phosphorus-modified ZSM-5 had better dispersion than did magnesium-modified ZSM-5 one which rather appeared as agglomerates.

6.2 Recommendations

From this experiment, we have expected to improve catalyst for light olefin production. Recommendations for the future work are the following.

1. The effect of species on the separated of ZSM/5 zeolite catalyst should be further investigated.
2. The effect of particle size on ZSM/5 zeolite catalyst should be studied.



ศูนย์วิจัยทรัพยากร
จุฬาลงกรณ์มหาวิทยาลัย

REFERENCES

- [1] Ladwig, P.K.; Asplin, J.E.; Stuntz, G.F.; Wachter, W.A.; Henry, B.E. US Patent 6,069,287. Exxon Research and Engineering Corporation 2000.
- [2] Dath, J.P.; Vermeiren, W.; Herrenbout, K. WO 00/78894. Final Oil and Chemical Corporation 2000.
- [3] Barthoment, D. Acidic catalysts with Zeolites. Zeolites Science and Techonology: Matinus Nijhoff Publishers 1984.
- [4] Dath, J.P.; Vermeiren, J.W. WO 01/00749. Final Oil & Chemical Corporation.
- [5] Euro. Chemical News 69–1808 (1998) 39.
- [6] Carmen, G. Euro. Chemical News 72–1902 (2000) 46.
- [7] Cao, H.X. Chemical Industrial Engineering Progress (China) 22–9 (2003) 911.
- [8] Zhao, G.L.; Teng, J.W.; Song, Q.Y.; Xie, K.; Chen, Q.L. Production of propylene from C4 olefins by catalytic cracking. Petrochemical Technology 33 (2004): 100–103.
- [9] Gonzalez, M.R.; Kobe, J.F.; Fogash, K.B.; Dumesic, J.A. Promotion of n-Butane Isomerization Activity by Hydration of Sulfated Zirconia. Journal of Catalysis 160 (1996): 290-298.
- [10] Wang, L.; Xie, M.; Tao, L. Conversion of light paraffins for preparing small olefins over ZSM-5 zeolites. Catalysis Letters 28 (1994): 61-68.
- [11] Cañizares, P.; Lucas, A.D.; Dorado, F.; Pérez, D. Effect of zeolite pore geometry on isomerization of n-butane. Applied Catalysis A: General 190 (2000): 233-239.
- [12] Wakui, K.; Satoh, K.; Sawada, G.; Shiozawa, K.; Matano, K.; Suzuki, K.; Hayakawa, T.; Oshimura, Y.; Murata, K.; Mizukami, F. Cracking of n-Butane Over Alkaline Earth-Containing HZSM-5 Catalysts. Catalysis Letters 84 (2002): 259-264.
- [13] Jiang, G.; Zhang, L.; Zhao, Z.; Zhou, X.; Duan, A.; Xu, C.; Gao, J. Highly effective P-modified HZSM-5 catalyst for the cracking of C4 alkanes to produce light olefins. Applied Catalysis A: General 340 (2008) 176-182.

- [14] Wakui, K.; Satoh, K.; Sawada, G.; Shiozawa, K.; Matano, K.; Suzuki, K.; Hayakawa, T.; Yoshimura, Y.; Murata, K.; Mizukami, F. Dehydrogenative Cracking of n-Butane over Modified HZSM-5 Catalysts. Catalysis Letters 81 (2002): 83-88.
- [15] Ji, D.; Wang, B.; Qian, G.; Gao, Q.; Lu, G.; Yan, L.; Suo, J. A highly efficient catalytic C4 alkane cracking over zeolite ZSM-23. Catalysis Communications 6 (2005): 297-300.
- [16] Li, Y.G.; Xie, W.H.; Yong, Sh. The acidity and catalytic behavior of Mg-ZSM-5 prepared via a solid-state reaction. Applied Catalysis A: General 150 (1997): 231-242.
- [17] Krannila, H.; Haag, W.O.; Gates, B.C. Monomolecular and bimolecular mechanisms of paraffin cracking: n-butane cracking catalyzed by HZSM-5. Journal of Catalysis 135 (1992): 115-124.
- [18] Triantafillidis, C.S.; Evmiridis, N.P.; Nalbandian, L.; Vasalos, I.A. Industrial Engineering Chemistry 38 (1999) 916.
- [19] Xiang, T.L.; Sheng, W.L.; Song, X.M.; GuiFen, X.; Lin, W.X. New method for olefin production from light alkanes. Reaction Kinetics and Catalysis Letters 53 (1994): 205-209.
- [20] King, R.B. Encyclopedia of Inorganic Chemistry (1994) 4365.
- [21] Barrer, R.M. Hydrothermal Chemistry of zeolites. London: Academic Press 1982.
- [22] Bekkum, H.V.; Flanigen, E.M.; Jansen, J.C. STM image of silicalite-1 pore structure. Zeolites 11 (1991): 306-307.
- [23] Szoztak, R. Molecular Sieve Principle of Synthesis and Identification. New York: Van Nostrand Reinhold 1989.
- [24] Chen, D.; Moljord, K.; Fuglerud, T.; Holmen, A. The effect of crystal size of SAPO-34 on the selectivity and deactivation of the MTO reaction. Microporous and Mesoporous Materials 29 (1999): 191-203.
- [25] Sano, T.; Fujisawa, K.; Higiwara, H. High Stream Stability of H-ZSM-5 Type Zeolite Containing Alkaline Earth Metals Catalyst Deactivation. Studies in Surface Science and Catalysis 34 (1987): 613-624.
- [26] Ashton, A.G.; Batamanian, S.; Dwyer, J. Acid in Zeolite. Catalysis by Acid-Bases. Amsterdam: Elsevier 1985.
- [27] Satterfield, C.N. Heterogeneous Catalysis in Industrial Practice. New York: McGraw-Hill 1991.

- [28] Tanabe, K.; Misono, M.; Ona, Y.; Hattori, H. New Solid Acids and Bases. Studies in Surface Science and Catalysis 51 (1989): 1-369.
- [29] Zhu, X.; Liu, Sh.; Song, Y.; Xu, L. Catalytic cracking of C4 alkenes to propene and ethene: Influences of zeolites pore structures and Si/Al₂ ratios. Applied Catalysis A: General 288 (2005): 134-142.
- [30] Wang, B.; Gao, Q.; Gao, J.; Ji, D.; Wang, X. Synthesis, characterization and catalytic C4 alkene cracking properties of zeolite ZSM-23 Applied Catalysis A: General 274 (2004): 167-172.
- [31] Mao, D.; Yang, W.; Xia, J.; Zhang, B.; Song, Q.; Chen Q. Highly effective hybrid catalyst for the direct synthesis of dimethyl ether from syngas with magnesium oxide-modified HZSM-5 as a dehydration component. Journal of Catalysis 230 (2005): 140-149.



APPENDICES

ศูนย์วิทยทรัพยากร
จุฬาลงกรณ์มหาวิทยาลัย

APPENDIX A

SAMPLE OF CALCULATIONS

A-1. Calculation of Si/Al Atomic Ratio for ZSM-5

The calculations base on weight of sodium silicate ($\text{Na}_2\text{O} \cdot \text{SiO}_2 \cdot \text{H}_2\text{O}$) in B1 and B2 solution.

Molecular weight of Si	=	28.0855
Molecular weight of SiO_2	=	60.0843
Weight percent of SiO_2 in Sodium Silicate	=	28.5
Molecular weight of Al	=	26.9815
Molecular weight of AlCl_3	=	133.3405
Weight percent purity of AlCl_3	=	97

For example, to prepare MFI at Si/Al atomic ratio of 40

Using sodium silicate 69 g with 45 ml of water as B1 and B2 solution.

$$\begin{aligned} \text{Mole of Si used} &= \frac{\text{wt}(\%)}{100} \times \frac{(\text{M.W. of Si})}{(\text{M.W. of SiO}_2)} \times \frac{(1 \text{ mole})}{(\text{M.W. of Si})} \\ &= 69 \times (28.5/100) \times (1/60.0843) \\ &= 0.3273 \end{aligned}$$

Si/Al atomic ratio = 40

$$\begin{aligned} \text{Mole of AlCl}_3 \text{ required} &= 0.3273/40 \\ &= 0.0081825 \text{ mole} \\ \text{Amount of AlCl}_3 &= 0.0081825 \times 133.34 \times (100/97) \\ &= 1.1248 \text{ g} \end{aligned}$$

Which used in A1 an A2 solutions.

A-2. Calculation of The Amount of Magnesium Loaded to ZSM-5 Catalyst

Determine the amount of magnesium are used loading to catalyst by incipient impanation method and solid state ion exchange method.

The catalyst use = 0.1 g

For example, to prepare MgI/ZSM-5 at 1% wt magnesium loading.

The magnesium use = X

So that

$$\begin{aligned}\frac{X}{1+X} &= \frac{1}{100} \\ 99X &= 1 \\ X &= 1/99 = 0.01\end{aligned}$$

Use $\text{Mg}(\text{NO}_3)_2 \cdot 6\text{H}_2\text{O}$ (M.W.256.41)

$$\begin{aligned}\text{Weight of } \text{Mg}(\text{NO}_3)_2 \cdot 6\text{H}_2\text{O} &= 0.01 \times (256.41/24.3) \\ &= 0.1055 \text{ g}\end{aligned}$$

A-3. Calculation of The Amount of Phosphorus Loaded to ZSM-5 Catalyst

Determine the amount of magnesium are used loading to catalyst by incipient impanation method.

The catalyst use = 0.1 g

For example, to prepare PI/ZSM-5 at 1% wt magnesium loading.

The magnesium use = X

So that

$$\begin{aligned}\frac{X}{1+X} &= \frac{1}{100} \\ 99X &= 1 \\ X &= 1/99 = 0.01\end{aligned}$$

Use $(\text{NH}_4)_2\text{HPO}_4$ (M.W.130)

Weight of $(\text{NH}_4)_2\text{HPO}_4$ = $0.01 \times (130/31)$

= 0.0419 g



ศูนย์วิทยทรัพยากร
จุฬาลงกรณ์มหาวิทยาลัย

APPENDIX B

CALCULATIONS OF REACTION FLOW RATE

Sample of Calculation

The used catalyst = 0.3 g

Pack catalyst into stainless reactor (inside diameter = 0.7 cm)

Determine the average high of catalyst bed = 2.2 cm, so that

$$\text{Volume of bed} = (\pi/4)(0.7)^2 \times 2.2 = 0.8462 \text{ ml}$$

$$\text{GSHV} = \frac{\text{Volumetric flow rate}^1}{\text{Volume of bed}}$$

$$\text{GSHV} = \frac{2600 \text{ (ml/h)}}{0.8462}$$

$$\text{GSHV} = 3,073 \text{ h}^{-1}$$

At STP condition:

$$\text{Volumetric flow rate(At } T \text{ } ^\circ\text{C)} = \text{Volumetric flow rate}^1 \times \frac{(273.15 + T)}{273.15}$$

Where T = room temperature

APPENDIX C

DATA OF EXPERIMENT

Calculation of conversion and hydrocarbon distribution of butane conversion reaction

Butane conversion activity was evaluated in term of conversion of butane into other hydrocarbon

$$\text{Butane conversion (\%)} = \frac{(\text{Butane conversion}_{\text{in}} - \text{Butane conversion}_{\text{out}})}{\text{Butane conversion}_{\text{in}}} \times 100$$

Selectivity of product is defined as mole of product (HC) from with respect to mole of butane converted:

$$\text{Selectivity HC (\%)} = \frac{\text{mole of HC from}}{\text{mole of butane converted}} \times 100$$

Where HC is product, mole of HC can be measure employing the calibration curve of products.

ศูนย์วิทยทรัพยากร
จุฬาลงกรณ์มหาวิทยาลัย

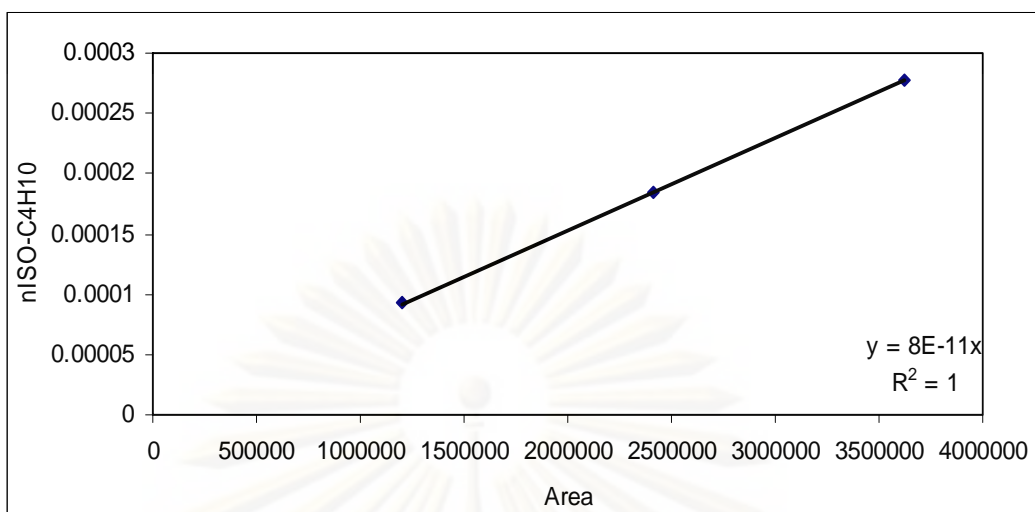


Figure C.1 The calibration curve of isobutane.

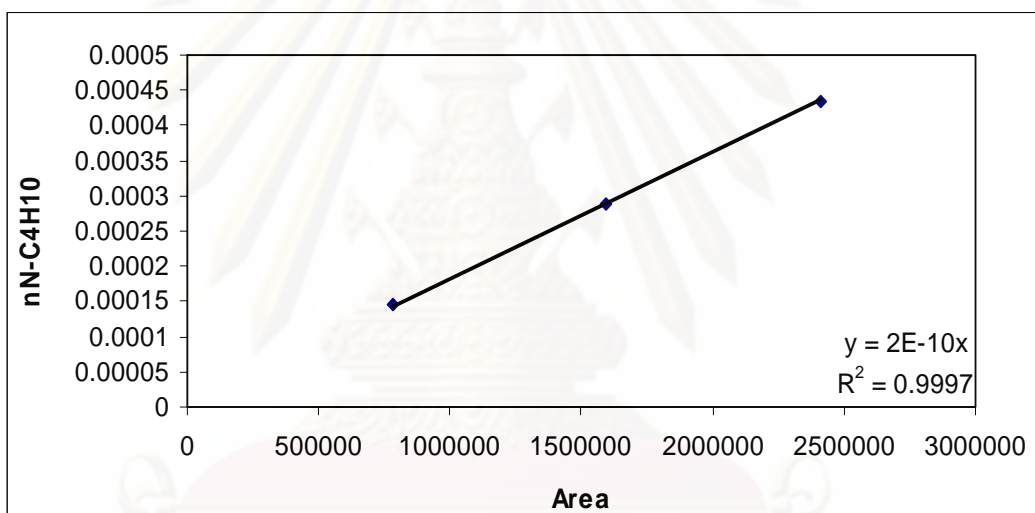


Figure C.2 The calibration curve of n-butane.

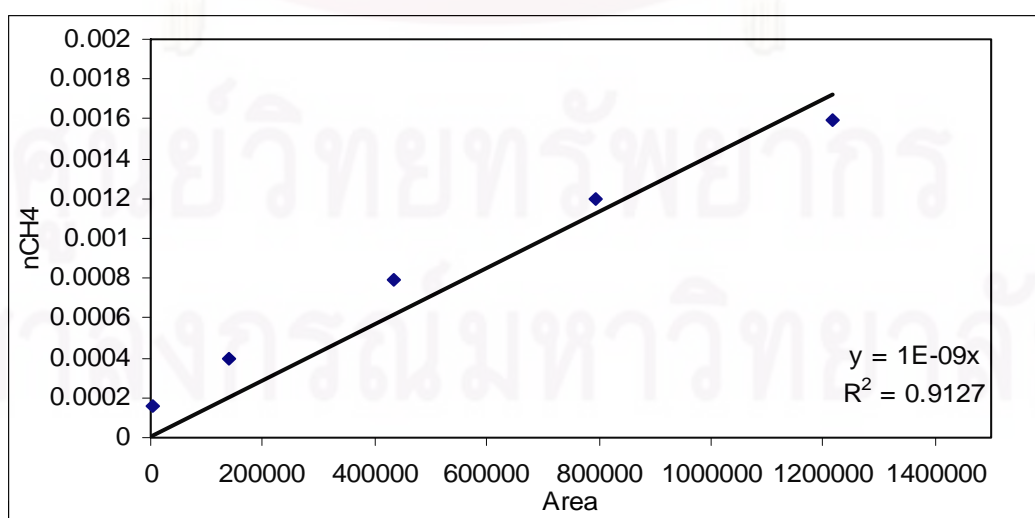


Figure C.3 The calibration curve of methane.

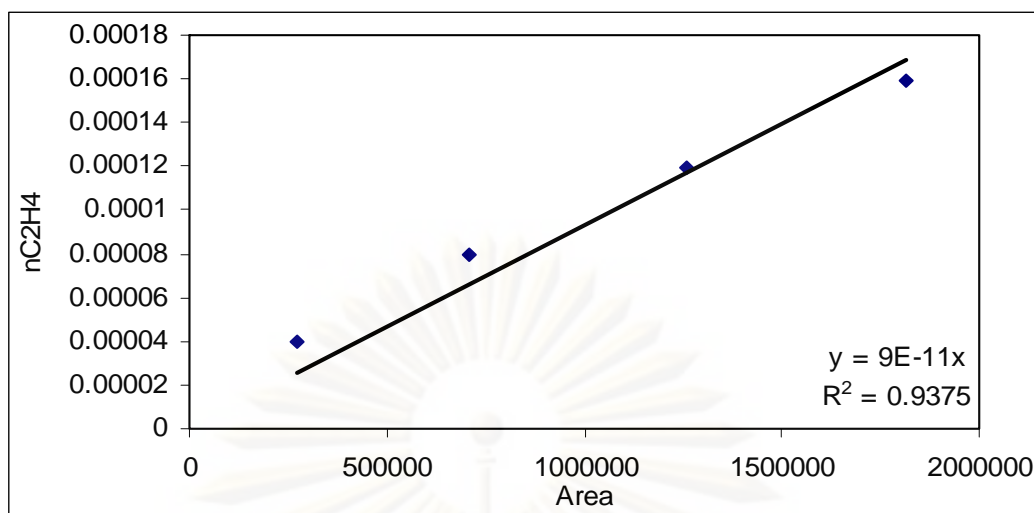


Figure C.4 The calibration curve of ethene.

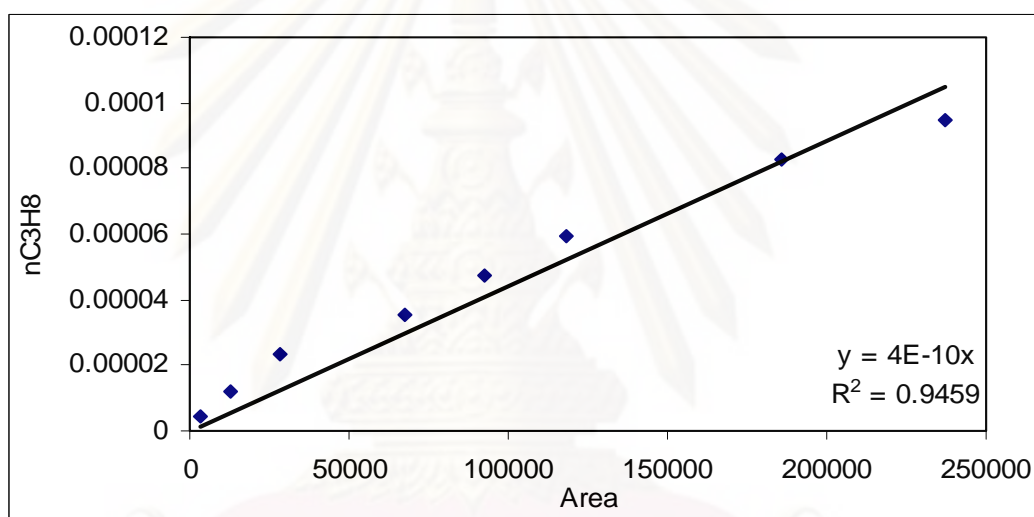


Figure C.5 The calibration curve of propane.

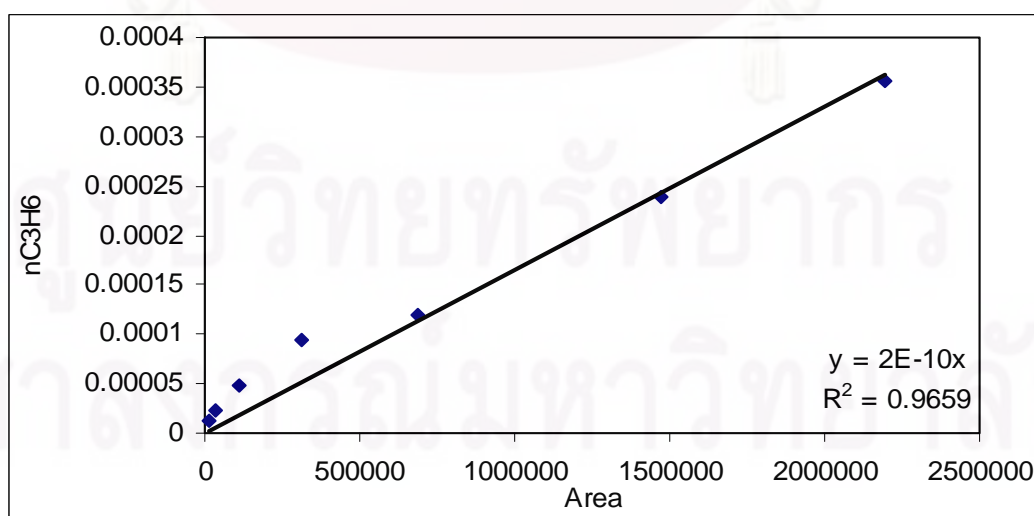


Figure C.6 The calibration curve of propene.

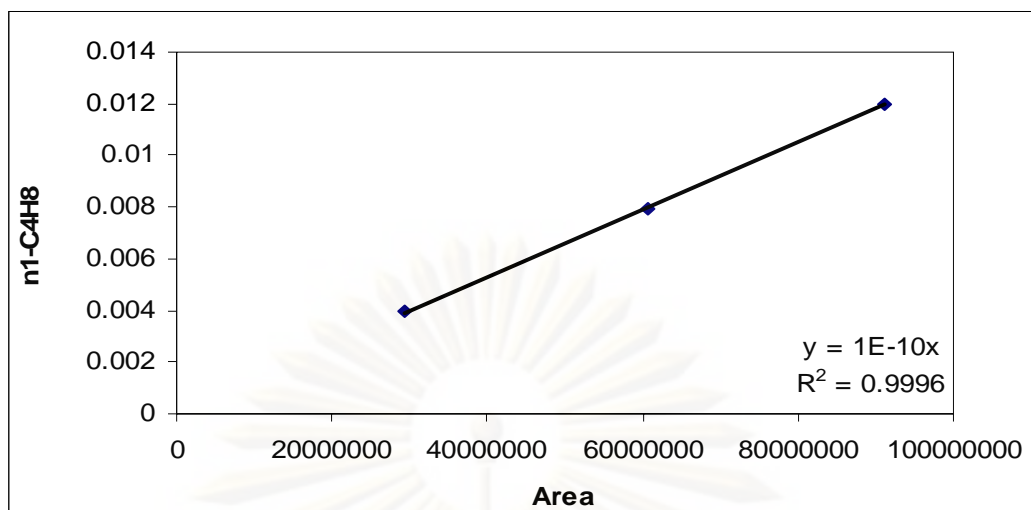


Figure C.7 The calibration curve of isobutene.

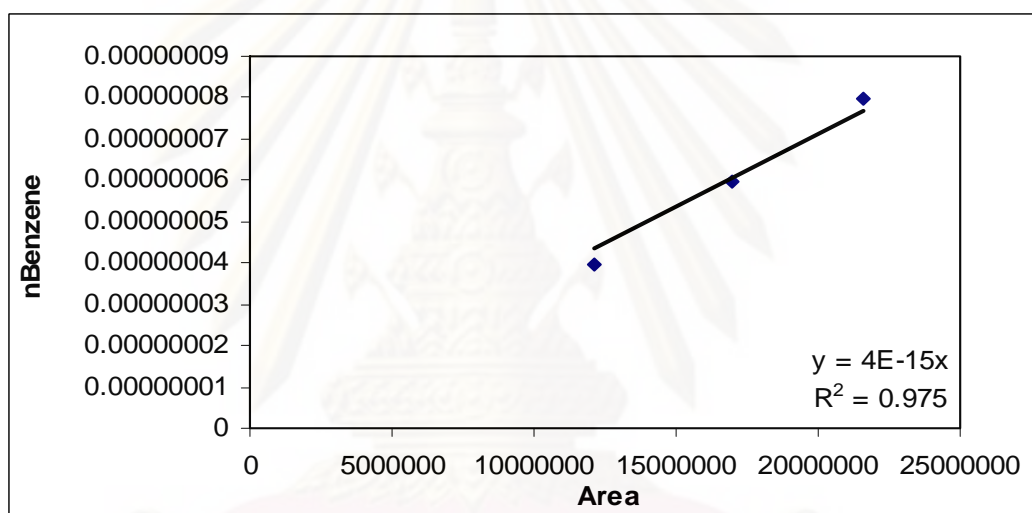


Figure C.8 The calibration curve of benzene.

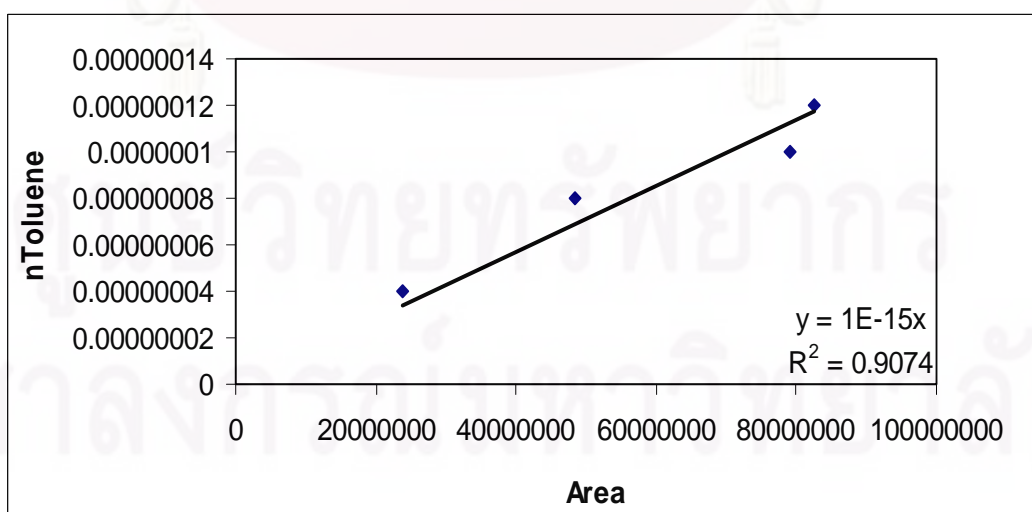


Figure C.9 The calibration curve of toluene.

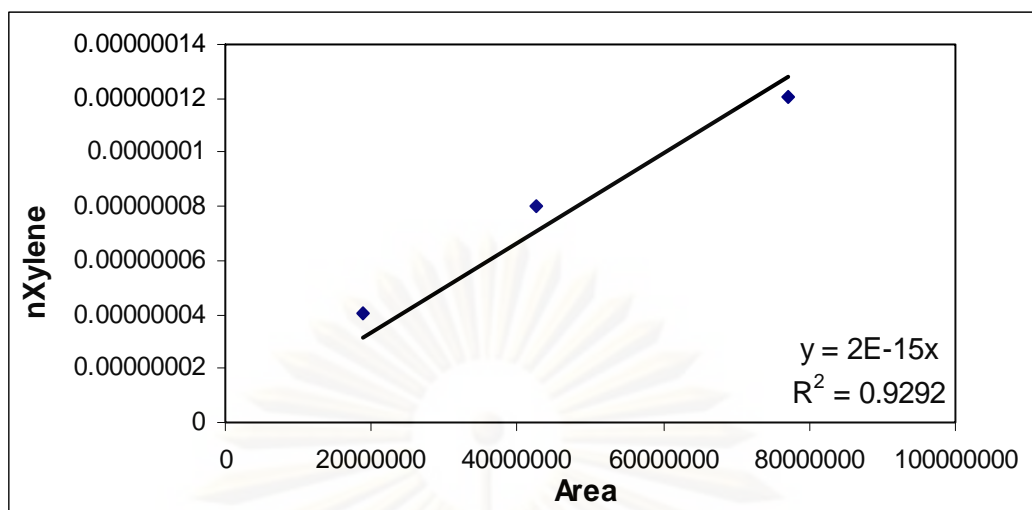
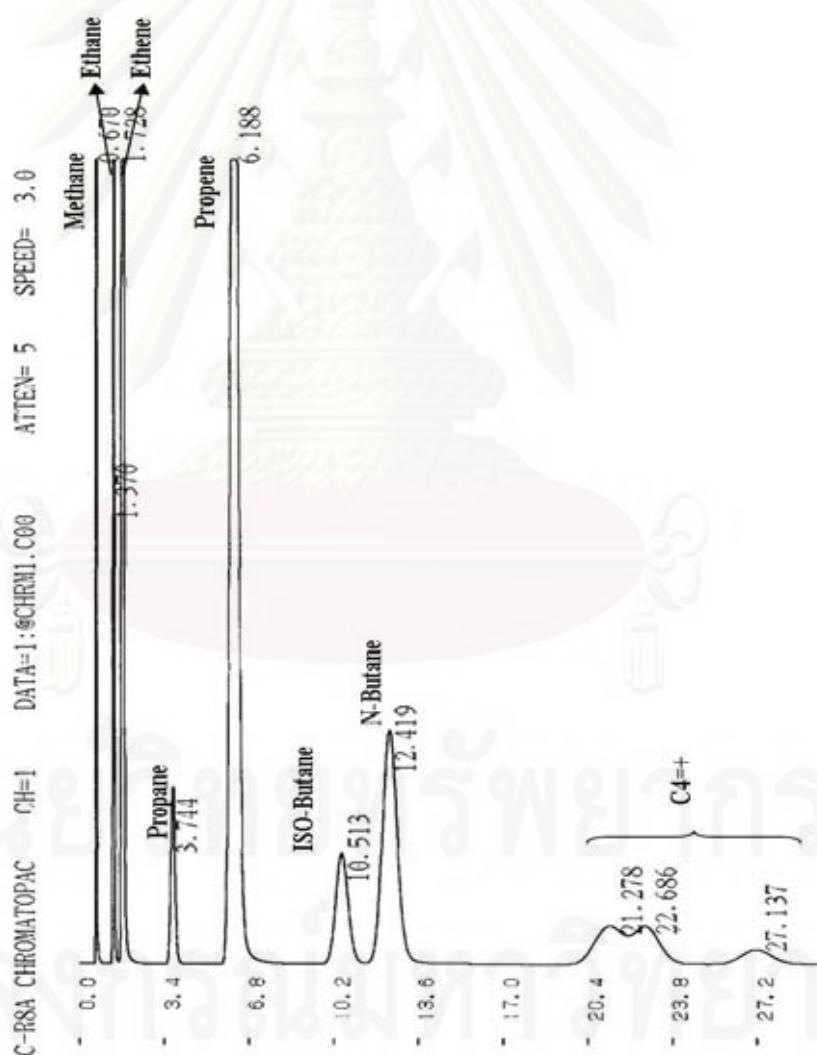


Figure C.10 The calibration curve of xylene

ศูนย์วิทยทรัพยากร
จุฬาลงกรณ์มหาวิทยาลัย

Table C.1 Condition uses in Shimadzu modal GC14B

Parameter	Condition of Shimadzu GC14B
Width	5
Slope	50
Drift	0
Min.area	1000
T.DBL	0
Stop time	30
Attend	5
Speed	3
Method	1
SPL.WT	100
IS.WT	1

**Figure C.11** The GC14B peaks of hydrocarbons

APPENDIX D

DATA AND CALCULATION OF THE ACID SITE

Calculation of total acid sites

For example, H-ZSM-5(40), total acid site is calculated from the following step.

1. Conversion of total peak area to total peak volume

Conversion factor from Micromeritics Chemisorb 2750 is equal to 77.57016 ml/ area unit. Therefore, total peak volume is derived from

$$\begin{aligned}\text{Total peak volume} &= 77.57016 \times \text{total peak area} \\ &= 77.57016 \times 1.071718 \\ &= 83.13334 \text{ ml}\end{aligned}$$

2. Calculation for adsorbed volume of 15% NH₃

$$\begin{aligned}\text{Adsorbed volume of 15\% NH}_3 &= 0.15 \times \text{total peak volume} \\ &= 0.15 \times 83.13334 \text{ ml} \\ &= 12.47 \text{ ml}\end{aligned}$$

3. Total acid sites are calculated from the following equation

$$\text{Total acid site} = \frac{(\text{Adsorbed volume, ml}) \times 101.325 \text{ Pa}}{(8.314 \times 10^{-3}, \text{ Pa}\cdot\text{ml}\cdot\text{K}^{-1}\cdot\mu\text{mol}^{-1}) \times 298 \text{ K} \times (\text{weight of catalyst, g})}$$

For H/ZSM-5(40) sample, 0.1 g of this one was measured, therefore

$$\begin{aligned} \text{Total acid site} &= \frac{12.47 \text{ ml} \times 101.325 \text{ Pa}}{(8.314 \times 10^{-3}, \text{ Pa}\cdot\text{ml}\cdot\text{K}^{-1}\cdot\mu\text{mol}^{-1}) \times 298 \text{ K} \times (\text{weight of catalyst, g})} \\ &= 4802 \mu\text{mol H}^+/\text{g} \end{aligned}$$



ศูนย์วิทยทรัพยากร
จุฬาลงกรณ์มหาวิทยาลัย

APPENDIX E

TETRAHEDRAL ALUMINUM OF ZSM-5 CATALYST

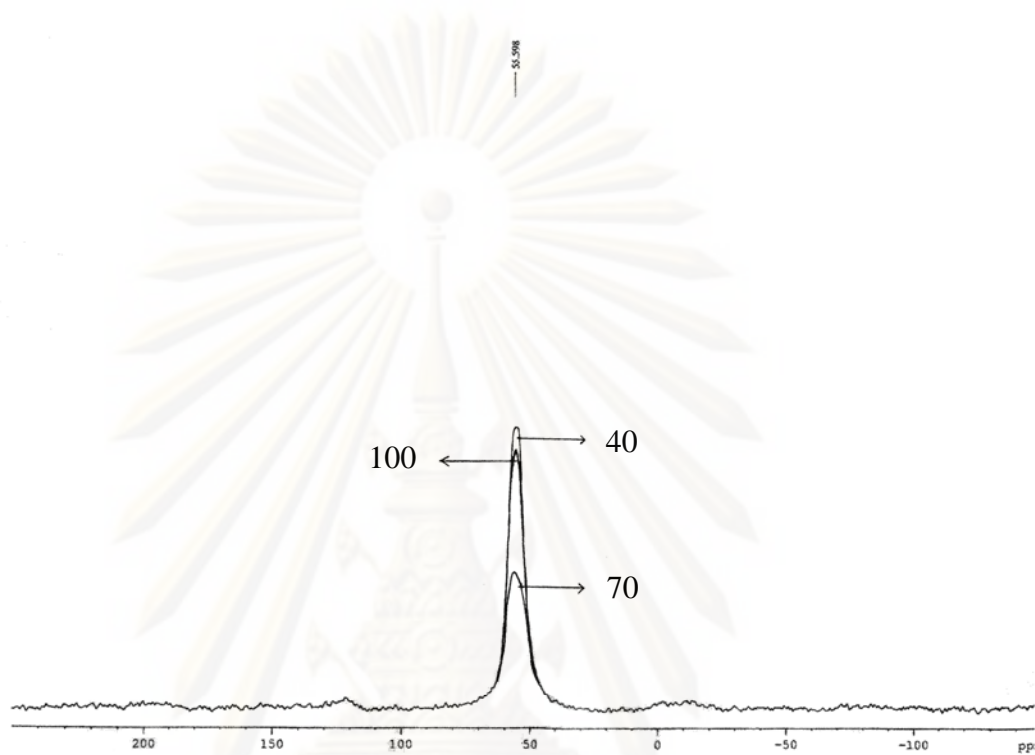


Figure E.1 The signal of alumina tetrahedral could be detected at around 54 ppm.

ศูนย์วิทยทรัพยากร
จุฬาลงกรณ์มหาวิทยาลัย

VITAE

Mr. Piyanun Phomthong was born in August 22, 1980 in Bangkok, Thailand. He received the Bachelor's Degree in Environmental Engineering from Department of Environmental Engineering, Faculty of Engineering, Chulalongkorn University in May 2004. He had worked in unicharm(Thailand). He entered the Master of Engineering in Chemical Engineering at Chulalongkorn University in June 2005.



ศูนย์วิทยทรัพยากร
จุฬาลงกรณ์มหาวิทยาลัย